

ABSTRACT

Title of Thesis: HUMAN-HUMAN SENSORIMOTOR INTERACTION

Sara Honarvar, Master of Arts,

Thesis Directed By: Dr. Jae Kun Shim, Ph.D.
Department of Kinesiology

We investigated the role of sensory feedback in inter-personal interactions when two co-workers are working together. Twenty-five co-workers completed two isometric finger force production experiments. In Experiment 1, co-workers isometrically produced finger forces such that combined force will match a target force and/or torque under different visual and haptic conditions. In Experiment 2, without participants' knowledge, each performed the same task with the playback of his/her partner's force trajectory previously recorded from Experiment 1. Results from both experiments indicated that co-workers performed the task worse in the presence of haptic and visual feedback. Since, in latter as opposed to the former condition, they adopted a compensatory strategy to accomplish the task accurately. Further analysis showed that co-workers achieved the same level of motor performance with similar control strategies, suggesting that they did not work synergistically to achieve better performance, but one co-worker processed another as disturbance when they worked together.

HUMAN-HUMAN SENSORIMOTOR INTERACTION

by

Sara Honarvar

Thesis submitted to the Faculty of the Graduate School of the
University of Maryland, College Park, in partial fulfillment
of the requirements for the degree of
[Master of Arts]
[2019]

Advisory Committee:

Jae Kun Shim, Ph.D., Chair

Hyun Joon Kwon, Ph.D.

Jin-Oh Hahn, Ph.D.

Yancy Diaz-Mercado, Ph.D.

© Copyright by
Sara Honarvar
2019

Table of Contents

Table of Contents	ii
List of Tables	iv
List of Figures	v
Chapter 1 : Introduction	1
1.1 General Introduction	1
1.2 Specific Aims and Hypotheses	3
Chapter 2 : Literature Review	9
2.1 Coordination in Human-Human Interaction	9
2.2 How Does CNS solve the degrees of freedom problem?	12
2.2.1 Optimal Control	12
2.2.2 Motor Synergy	13
2.2.3 The Uncontrolled Manifold Hypothesis (UCM).....	14
2.2.4 Hierarchical Control of Movement	15
Chapter 3 : How do task constraints affect co-working behavior?.....	17
3.1 Abstract	17
3.2 Introduction.....	17
3.3 Methods.....	21
3.3.1 Participants.....	21
3.3.2 Equipment	21
3.3.3 Procedures.....	22
3.4 Data Analysis	25
3.4.1 Hierarchical Variability Decomposition (HVD).....	25
3.4.2 Statistics	27
3.5 Result	28
3.5.1 Force trajectories.....	28
3.5.2 HVD for HHI	28
3.5.3 The role of task constraints in inter-personal motor performance and synergy	29
3.6 Discussion	33
3.6.1 The role of task constraints in co-working behavior	33
3.6.2 The role of task constraints in intra-personal synergy	36
3.7 Conclusion	37
Chapter 4 : Do we work together synergistically?	38
4.1 Abstract	38
4.2 Introduction.....	38
4.3 Methods.....	41
4.3.1 Participants.....	41
4.3.2 Equipment	41
4.3.3 Procedures.....	42
4.4 Data Analysis	46
4.4.1 Hierarchical Variability Decomposition (HVD).....	46

4.4.2 Statistics	49
4.5 Result	49
4.5.5 Characterization of Inter-personal Motor Synergy	49
.....	52
4.6 Discussion.....	53
4.6.1 Characterization of the co-working behavior	53
4.6.1 Spectral Analysis	55
4.7 Conclusion	62
Chapter 5 : A feedback control model with Bayesian multisensory integration that simulates multi-finger synergy during constant finger force production.....	63
5.1 Abstract.....	63
5.2 Introduction.....	63
5.3 Methods.....	66
5.3.1 Multi-Digit Finger Force Production: Experimental Data.....	66
5.3.1.1 Participants.....	66
5.3.1.2 Experimental setup.....	67
5.3.2 Multi-Digit Finger Force Production: Mathematical Model	68
5.3.3 Multi-Digit Finger Force Production: Simulation	73
5.3.5 The role of tactile sensory feedback in multi-finger synergy	76
5.3.5 Data Analysis	77
5.4 Results.....	79
5.4.1 Finger Force Trajectories	79
5.4.2 Synergistic Interaction between fingers through HVD analysis	79
5.5 Discussion.....	80
5.6 Future Directions	82
Appendices.....	84
Relation between HVD and Uncontrolled Manifold	84
Personality Questionnaire	86
Predicting closed-loop behavior from open-loop conditions.....	86
Bibliography	88

This Table of Contents is automatically generated by MS Word, linked to the Heading formats used within the Chapter text.

List of Tables

Table 3.1. Different Conditions of Human-Human Interaction (HHXX) in Experiment I	24
Table 4.1. Different Conditions of Human-Data Interaction (HXD) in Experiment II	44

List of Figures

Figure 3.1. Experiment apparatus: a) Experimental setting. b) Customized seesaw with force sensors when it is freely moving about its axis of rotation. c) Customized seesaw with force sensors when it is mechanically fixed. d) Continuous visual feedback of the real-time force data, e) Instantaneous visual feedback of the real-time force data	22
Figure 3.2. Hierarchical organization of dyadic performance in a redundant multi-finger force matching task	27
Figure 3.3. Force trajectories in a hierarchical manner for a representative pair in a) HHMC condition and b) HHFC condition. In both figures, bottom figure (intra-personal level) represents the forces recorded from individual index (I) and middle (M) fingers. The mid-level (inter-personal level) shows sum of index and middle finger forces produced by person one (P1) and person two (P2). Finally, the top level, task level, demonstrates sum of forces produced by two persons.	28
Figure 3.4. HVD analysis for different conditions of HHI experiment. The gray and pink bars show instantaneous condition, respectively.	32
Figure 3.5. Comparing HHFC condition with HSD and HCD conditions	33
Figure 3.6. Task constraints and DOF in a) Fixed and b) Moving conditions	34
Figure 4.1. Experiment apparatus: a) Experimental setting. b) Customized seesaw with force sensors. c) Continuous visual feedback of the real-time force data.....	42
Figure 4.2. Demonstration of the visual feedback that participants receive in a) HHI experiment, and b) HSD condition of experiment II. Letter F denotes each participant’s force at current time while letter SD represents the solo part of data recorded from HHI experiment.	45
Figure 4.3. Demonstration of the visual feedback that participants receive in a) HHI experiment, and b) HCD condition of experiment II. Letter F denotes each participant’s current force while letter CD represents the co-working part of data that was recorded from HHI experiment.	46
Figure 4.4. Hierarchical organization of dyadic performance in a redundant multi-finger force matching task	48
Figure 4.5. Hierarchical structure for human working with a) human co-worker, and b) non-human co-worker (working with solo part (SD2) or co-working part (CD2) of their partner’s data).....	49
Figure 4.6. Comparing HHI with HSD and HCD conditions	52
Figure 4.7. a) two-way connection between co-workers in HHI b) one-way connection between person and data (input-output mapping between visual sensory disturbances and force of the person in response to the disturbance), the same mapping can be formed for P2.	55
Figure 4.8. Comparing the PSDs of two different inputs. Input in HSD condition was solo part of data recorded from HHI (SD2) and HCD condition it was co-working part of data recorded from HHI (CD2).	57
Figure 4.9. comparing the conditioned PSD for HSD and HCD conditions	58
Figure 4.10. The gain and phase of FRF in HSD and HCD conditions	59
Figure 4.11. Predicting co-working behavior from open-loop conditions.....	61
Figure 5.1. Experimental Setting	67

Figure 5.2. The proposed feedback control model block diagram for finger force production task	69
Figure 5.3. Schematic of CBC model taken from ⁸⁶	70
Figure 5.4. Complex coherence. a) magnitude squared coherence. b) phase of complex coherence	75
Figure 5.5. Equivalent feedback control block diagram of the multi-digit finger force production task in the (a) absence (b) presence of tactile sensory feedback	77
Figure 5.6. Simulated and experimental resultant (i.e., black line) and individual finger forces for a) presence of tactile feedback, b) absence of tactile feedback. In both conditions, the solid lines represent the experiment and the dash lines represent the simulation	79
Figure 5.7. The HVD analysis for the experiment and simulation. The blue bars show the presence and the red bars show the absence of tactile feedback.....	80

Chapter 1 : Introduction

1.1 General Introduction

Inter-personal interactions are frequent in our everyday lives such as shaking hands, lifting and carrying heavy objects with a friend, assisting a child riding a bicycle, playing games, etc. To ensure that two or more people can perform a task accurately and successfully, they need to coordinate with each other appropriately. They could not achieve this coordination unless they adapt, anticipate, and react to each other's forces and movements suitably. The term, joint action, has been recently used to describe this sort of interactions which is defined as: "... an interaction between two or more individuals that coordinate their actions in space and time to bring about a change in the environment"¹. Over the past decade, there has been a growing interest in understanding the mechanism underlying joint actions¹⁻⁹ due to its application to many fields such as human-robot collaboration and rehabilitation. Most of these applications require physical interaction between partners. However, despite its importance, our knowledge of the role of physical interaction on the inter-personal motor performance and motor coordination is limited.

Physical interaction (or haptic interaction) is defined as joint actions arising from physical coupling between effectors of one agent or effectors of two or more agents. Physical interactions can be intra-personal, e.g., manipulating an object using two hands, or inter-personal, e.g., carrying an object with another person. In both cases, the achievement of a successful motor task requires coordination between the effectors. Intra-personal coordination is known to be established by the central nervous system (CNS) for overcoming the inherent redundancy (i.e., having more degrees of freedom (DOF) than necessary for particular task performance in the system¹⁰⁻¹³). One of the major questions in motor control is how CNS manages to select a solution from many "apparently" similar alternatives for performing a motor task and overcome the issue of redundancy. Theory of

motor synergies is one of the many proposed solutions to this issue¹⁰⁻¹³. This theory states that having many DOF for performing a task is providing CNS with more flexibility. In this case, CNS is not required to select a single motor effector from many to stabilize the task performance, but it instead uses a family of solutions (known as motor synergies) to deal with potential perturbations¹². In this case, when one effector/element causes an error in the performance, the other effector/element changes its behavior in a way that compensates the error.

The observation of pairs of individuals being able to produce coordinated movement and compensate for each other's error suggests that we might be able to extend the notion of motor synergies to joint actions^{14,15}. However, in this case, in the absence of a central controller, non-centralized processes such as dynamical mechanisms emerging from the visual or haptic interaction between agents could be responsible for the inter-personal coordination. Unlike the intra-personal coordination, the underlying mechanism of inter-personal coordination, where even more degrees of freedom have been introduced to the system, has remained unknown.

The established coordination between partners may occur spontaneously or intentionally with an action plan¹⁶⁻¹⁸. For example, some studies have shown that when two people perform a task while observing each other's behavior, they fall into the same rhythm without prior intention^{14,15,19,20}. While some other studies provided some evidence that people would adjust their actions to those of their partner as they receive sensory information from them such as visual²⁰, haptic²¹, or auditory^{3,22}. Masumoto and Inui studied coordination in joint actions through a periodic isometric finger force production task⁴. They asked participants to produce forces such that the sum of their forces was a target force while receiving the visual feedback of combined force and the target on a monitor in front of them. They observed a high negative correlation between forces produced by individuals and time-synchronized force outputs. These results indicate the adoption

of simultaneous complementary and synchronous strategies by partners for the facilitation of the coordination between them.

Studies on within-person interlimb coordination show that there is a close relationship between redundancy and hierarchical structure of motor control^{13,23,24}. This type of control suggests that the distribution of the task across different levels in a hierarchy results in decreasing the variables manipulated by a higher level of control and alleviates the problem of motor redundancy. In a recent study⁵, the hierarchical structure of motor control was tested in a joint action that involved bimanual force production. Participants were asked to work as a pair or individually to produce forces such that the sum of their forces was a target. They observed that turning an individual bimanual force production task into a joint force production task would result in positive correlation (synchronous strategy) between forces produced by two hands of individuals to enable negative correlation (complementary strategy) between two participants' forces. They also showed that the variability of human actions is smaller inter-personally than individually due to the emerged coordination between them. In an earlier study conducted by the same group, they showed that this coordination was established as a result of the visuomotor linkages between participants⁴.

In the present study, we examined how physical interaction between participants would influence the hierarchical organization of motor control in a bimanual joint action by extending a previously developed hierarchical variability decomposition (HVD)²⁵ method to joint actions.

1.2 Specific Aims and Hypotheses

Aim 1. To investigate the role of visual feedback of combined motor outcome presented to co-workers in their inter-personal synergy and motor performance (Experiment I: Human-Human)

It is well documented that the visual feedback of the overall output plays an essential role during intra-personal²⁶ and inter-personal motor tasks²⁷. Previous studies have shown that the intermittency of feedback^{28,29} and visual manipulation of the output³⁰ would modulate performance outcome in bimanual tasks. However, no study to our knowledge has investigated how the inter-personal motor performance and coordination are affected by the extent to which the visual information of motor output is being provided to them. In other words, it is unknown whether or not having access to information about the whole time-course of motor output (past as well as current states) versus current states only would alter the inter-personal motor performance and synergy.

Hypothesis 1.1: Inter-personal synergy exists when visual feedback of combined motor outcome is presented to co-workers

Hypothesis 1.2: Presenting the continuous time trajectory of combined motor outcome improves inter-personal motor performance

Task 1.1: Two subjects were asked to work as a pair to complete a target-tracking task while being physically connected through a customized seesaw-lever structure. They were instructed to rest the index and middle fingers of their right hand on force sensors placed on the seesaw and start pressing after hearing an auditory cue. Their task was to match the combined force to a target line, both of which were shown on a monitor in front of them. In this task they were receiving two different visualization of the real-time force data: a) the whole course of force trajectory is presented to them (i.e., Continuous condition), showing the force produced at past states as well as current state, and b) only current force data is shown (i.e., Instantaneous condition).

Dependent variables: OMSE, covariance between forces produced by dyads

Expected outcomes:

- 1) **OMSE for the Continuous condition would be smaller than Instantaneous condition.**
- 2) **Covariance would be negative for both conditions, and it will be larger in magnitude for the Continuous condition compared to the Instantaneous.**

Poulton³¹ showed that performance was improved when the feedback information about past states of the pathway, in a sine wave-like target tracking task, was given to participants. He concluded that information about the past states of the target allowed the participants to predict future states of the target path better. We speculated that in joint actions if two people are provided with the visual feedback information of the joint behavior in the past and current states, they can coordinate their actions better and perform the task more accurately. Because, they can integrate the information from past to present state and reduce the uncertainty in task performance. Also, according to previous studies^{4,5,27,32-34}, having the visual feedback of combined motor outcome induces synergistic interaction between co-workers.

Aim 2. To investigate the role of visual feedback when accompanied with haptic feedback in inter-personal synergy and motor performance (Experiment I: Human-Human)

Some behavioral studies have provided evidence that the presence of haptic feedback exchanged between partners in addition to visual feedback would improve inter-personal visuomotor task performance as compared to conditions where only visual feedback is available^{1,9,21,35,36}. However, our knowledge of the underlying neural control mechanism behind this improvement has remained shallow. Moreover, it is not clear how the presence of physical linkage between two people would alter the motor synergy between them. Thus, aim 2 examines the effect of haptic feedback exchanged between two people on their inter-personal motor performance and synergy according to the HVD analysis.

Hypothesis 2.1: Adding haptic feedback exchanged between co-workers to visual feedback improves inter-personal synergy.

Hypothesis 2.2: Adding haptic feedback exchanged between co-worker to visual feedback improves inter-personal motor performance

Task 2.1: Two subjects were asked to work as a pair to complete a target-tracking task while being physically connected through a customized seesaw-lever structure. They were instructed to rest the index and middle fingers of their right hand on force sensors placed on the seesaw and start pressing after hearing an auditory cue. Their task was to match the combined force to a target line, both of which are shown on a monitor in front of them. They performed this task under two conditions: a) when the seesaw-lever was moving (i.e., Moving condition) and b) when it was mechanically fixed (i.e., Fixed condition). During the experiment, they were blocked from the view of each other and not allowed to talk to each other.

Dependent variables: OMSE, covariance between forces produced by two participants

Expected outcomes:

- **OMSE for the moving condition would be smaller than the fixed condition.**
- **Covariance would be negative, and it will be larger in magnitude for the Moving condition compared to the Fixed.**

According to the previous studies^{37,38} the availability of an additional source of information (i.e., haptic feedback) besides the visual feedback to dyads decreases the uncertainty in the task performance and allows the emergence of a sense of “togetherness” between partners³⁸. Furthermore, we speculate that in both conditions partners would take compensatory strategy (i.e., negative covariance), meaning that if one person introduces an error to the task performance, the other tries to compensate for that error^{4,5,7,27}. We hypothesize that the compensatory strategy would

arise as a result of high coordination established due to visual and/or haptic linkages between the co-workers.

Aim 4. Characterization of Inter-personal Motor Synergy (Experiment II: Human-Human VS. Human-Data)

When people perform a motor task individually, CNS deals with noise and instabilities by coordinating muscle activations or effectors and produces synergistic interaction between them³⁹. We aim to examine if two people carry out a joint action while provided with some information on the joint task (e.g., through visual feedback), they would be able to coordinate with each other and produce synergistic interaction, as in the individual case. In other words, we would like to examine whether inter-personal motor synergy exists or not. Moreover, this synergy is formed due to a two-way connection and interaction between co-workers.

Hypothesis 4.1: We hypothesize that inter-personal motor synergy exists

Task 4.1: Participants repeated the same above-mentioned target tracking task in the condition that the seesaw was Fixed, and they received Continuous visual feedback of the force. They performed this task under two conditions: either as a pair or with the playback of their partner's force data, that was produced previously in experiment I, (i.e., Human-Data). In Human-Data condition, each co-worker worked with the data produced by his/her partner in previous Human-Human task trials. So, in this case, each partner worked with an open-loop signal. Note, that Human-Human experiment happened before Human-Data experiment.

Dependent variable: OMSE, covariance between forces produced by dyads

Expected outcome:

- **OMSE for Human-Human condition will be smaller than Human-Data condition**

- **The covariance between partner's force in Human-Human condition will be negative, but it will be zero in Human-Data condition.**

When two people are asked to complete a joint motor task and provided with some information on the joint action (e.g., visually), they are creating a closed-loop feedback system, and a two-way connection will be formed between them. Using the information exchanged between them, they try to anticipate their partner's action and react to it in a way that ensures high accuracy. The covariance between partner's force, in the Human-Human experiment, will be negative, representing that dyads are trying to overcome the redundancy by creating synergistic interaction^{7,27,34,40,41}. The covariance between a person's force and data in Human-Data experiment will be zero, representing that there is no synergy between person and data. The trajectory-playback will present a one-way connection where a subject could feel and respond to his partner's action, but the partner (whose data was recorded in the previous experiment) could not do the same. So, they will work independently of each other. In addition, since the data acts as an environmental disturbance, in order for the person to deal with this source of noise, synergistic interaction will emerge at intra-personal level¹¹; so, the covariance between the index and middle finger forces will be negative.

Chapter 2 : Literature Review

2.1 Coordination in Human-Human Interaction

Over the past decade HHI has been investigated through various tasks^{1,3-8,17,18,21-22,26-28,31,38,41-51}, a majority of which were visuomotor tasks. However, our understanding of the underlying mechanism behind physical HHI is still limited. In addition, it is known that completion of a joint action requires proper coordination between two people as they need to predict their partner's action and react to it suitably. Proper coordination can emerge according to the sensory information exchanged between them. Despite the growing body of research in the field of HHI, it is still unclear what kind of neural strategies people use to coordinate with each other and how this coordination is affected by the sensory information exchanged between them. Thus, the proposed study aims to address these issues.

According to HHI studies, control of joint actions can take any of “distributed” or “redundant” forms⁴⁷. In distributed control, as derived by its name, control is distributed among two or more people where they perform complementary actions to complete a task, for example when two people hold opposite ends of a table. In this type of actions, the distribution of control is predetermined from the outset by task constraints, and there is no freedom in adopting and adapting customized control strategies. In contrast, in redundant control, both partners have the same action possibilities, and they can distribute control freely. An example of these kinds of control could be pulling a rope in the same direction performed by two or more people. Independent of the type of task control, people need to coordinate their actions with their partner to assure a successful task performance¹. To do so, they may take on compensatory, synchronous, or both strategies⁴ according to the nature of the task and availability of the information about partner's action²¹.

Masumoto and Inui^{4,5} found that in a periodic finger force production task, two persons (dyads) perform better than individuals by adopting both compensatory and synchronous strategies. In their experiment, dyads were asked to reproduce a target force (by pressing on force sensors) which varied periodically over time. They were receiving a visualization of the target force and the combined force that they were producing on a monitor in front of them. Similar to the study conducted by Reed and colleagues³⁵, the forces produced by each individual in the joint condition were negatively correlated, indicating that participants adopted the compensatory strategy to perform the task. So, when one actor increased the exerted force, the other decreased his/her force to decrease the deviation from the target force. They showed that adopting this strategy allowed dyads to perform better than individuals.

Similarly, Reed and Peshkin³⁵ showed that when two participants are instructed to rotate a crank together to reach a moving target, they perform faster than working alone. They related this improvement in performance to the haptic communication between dyads. Equivalently, Ganesh and colleagues¹⁸ demonstrated that dyadic performance was better than solo performance in tracking the same moving target. However, a potential confounding factor of these studies could be that in the single-agent tasks, subjects performed the task unimanually, while the dyadic configuration involved two hands/arms that are both physically contributed to the task. So, it is not clear that the enhanced performance is due to an addition of an end-effector or the existence of inter-personal coordination and the physical coupling between two agents. There are very limited studies that have considered this issue. For instance, Van der wall and colleagues²¹ compared the motor output of two-agent with bimanual single-agent configuration and showed that dyads perform at the same level as individuals. They showed that dyads amplify their forces to coordinate with each other through the haptic channel dictated by the physical coupling between participants.

However, their task did not allow them to systematically test the effect of haptic feedback on performance, as they did not include a condition where only visual feedback is presented to pairs. Intuitively and from studies on intra-personal actions, one may think that more sensory information would be beneficial for accurate task performance as people tend to integrate various sensory information in an optimal fashion⁵¹ when they perform actions individually. However, the usefulness of information from multiple modalities in inter-personal activities needs to be further evaluated. Thus, the proposed study aims to investigate the role of haptic feedback exchanged between partners in control of a redundant task.

Furthermore, few studies have investigated the coordination between two people in relation to inherent redundancy in the human body and hierarchical structure of motor control⁴⁰⁻⁴². Humans have a complex body structure with typically more degrees of freedom (i.e., motor effectors) than is required for a successful task performance¹³. In general, the human body has hundreds of muscles which can act upon the skeleton and cause movement of joints and limbs. However, each active joint, limb, or segment, can also move in a variety of positions with a variety of velocities to accomplish the desired task²⁴. So, CNS faces with apparently redundant degrees of freedom (DOF) or motor elements as well as many options for varied patterns of muscle activation, kinematics, and kinetics to perform a successful movement. Therefore, theoretically each motor task can be performed in an endless number of ways⁵². Although all of these endless options are resulted in the same motor output, none of them are identical, which leads to a relatively high variability at elemental variables and low variability at the level of performance variables^{13,53}. Bernstein expressed this phenomenon as “repetition without repetition”¹³, meaning that each repetition of the same task is performed by unique neural and motor patterns.

One of the biggest issues in motor control is that how CNS manages to select a solution from many apparently similar alternatives for performing a motor task¹³. Within the context of the DOF problem, completing a motor task with a co-worker introduces even more DOF to the system. How two CNS collaborate with each other to handle this redundancy in the system is the basic question of the present study which also has become as one of the growing research interests in many fields such as motor control, neuroscience, and robotics^{1,4-7,19,27,28,31,43,46,47,50,51,56}.

2.2 How Does CNS solve the degrees of freedom problem?

2.2.1 Optimal Control

There have been many attempts to answer the DOF problem and to explain motor coordination. One of them is the theory of optimal control, which is based on the notion that CNS optimizes movement behavior with respect to the given task. This theory states that CNS tries to minimize/maximize a cost function (for example, minimization of energy expenditure) in order to find an optimal, single solution for achieving the goal of the task⁵⁵. Although there has been some evidence for supporting this theory, finding the cost function that CNS optimizes is very challenging and controversial.

Therefore, a more well-defined theory, the theory of optimal feedback control, associated with the mentioned theory, was proposed⁵⁶. Unlike the previous theory, this one suggests that CNS does not look for a single, optimized solution for the task, but it rather utilizes sensory feedback more “intelligently” to correct for only those deviations that interfere with successful task performance^{56,57}. This theory supports the high trial-to-trial variability that has been revealed in empirical studies by providing a range of solutions to a given motor task across multiple repetitions. This family of solutions is also known as motor synergies originally proposed by

Bernstein, which are organized through the pattern of co-variation of elemental variables that satisfies the task constraints¹³.

2.2.2 Motor Synergy

Bernstein suggested that CNS utilizes the many DOF to handle possible perturbations sensed by sensory system¹³, the idea that later led scientists to redefine the term redundancy to abundance which assures both stability and flexibility of performance²³. Therefore, when the sensory system senses a discrepancy between the desired and actual motor outputs, the CNS would try to correct for those errors that intervene successful task performance (also known as task-relevant variability) by making changes in the motor outputs. For example, when a pianist tries to play a constant sound but detects a deviation between the sound produced and the desired sound, he/she makes changes in muscle activation to correct for the error and plays the desired sound. The similar case in the laboratory settings would be asking subjects to produce a constant force of 10N by pressing the index and middle fingers of one hand on force sensors while showing them their produced force as well as the target force on a monitor in front of them. In this situation, it turns out the subject would try to minimize the deviation from the target force by changing the combinations of finger forces (i.e., reducing the force produced by one finger and increasing the force produced by the other to compensate for that reduction³⁹).

It is evident that there is an infinite number of finger force combinations that CNS could utilize to perform the mentioned motor task successfully. Therefore, according to motor synergy theory, CNS does not look for a single motor effector from many to stabilize the task performance, but it instead uses a family of solutions (e.g., different finger force combinations); motor synergies, to deal with potential perturbations. Synergy in the Oxford dictionary is defined as: “the interaction of two or more organizations, substances, or other agents to produce a combined effect greater

than the sum of their separate effects”. In motor control, an interaction is called synergistic if it has three essential characteristics: 1) Sharing: if elements of the movement system are organized in synergy, they should represent shared activity pattern of covariation. 2) Error compensation: if an element introduces an error into motor output, other elements will change their contribution in a way that minimizes this error²³ and ensures a stable (repeatable) task performance. 3) Task-dependence: synergistic organization of elements is specific to the task that they are performing. For example, different synergy can be created with the same set of elements to fulfill a specific functional purpose which allows stable and flexible task performance.

2.2.3 The Uncontrolled Manifold Hypothesis (UCM)

Scholz and Schoner³¹ introduced an approach called uncontrolled manifold (UCM) for quantification of synergy and the intrinsic variability in human movements. Within the UCM approach motor variability is decomposed into task-relevant (variability that affects performance error) and task-irrelevant dimensions (variability that does not interfere with the task performance)^{7,31}. Take the example of multi-finger force production task; the UCM approach would quantify the variance of individual finger forces (aka elemental variables) with respect to the variance of the sum of the individual finger forces, or the variance of total force produced (aka performance variable). The variance of the elemental variables is assigned to two separate subspaces: the UCM subspace that corresponds to a constant value of the total force and wherein changes do not affect overall task performance, and a subspace orthogonal to the UCM that corresponds to changes in the total force. The UCM subspace contains task-irrelevant variability, and CNS allows high variability within the UCM space, creating more flexibility for task performance. However, CNS restricts variability of elements outside this space if it intervenes the successful task performance⁵⁸.

The UCM hypothesis allows for an operational definition of motor synergy: if the variance within the UCM subspace (V_{UCM}) is larger than the variance within the space orthogonal to the UCM (V_{ORT}) then it can be concluded that a synergy exists³¹. The index of synergy (ΔV) is computed by taking the difference between V_{UCM} and V_{ORT} and normalizing it by the total variance in the system (V_{TOT}) per degrees of freedom using the following equation:

$$DV = \frac{V_{UCM} / n_1 - V_{ORT} / n_2}{V_{total} / (n_1 + n_2)} \quad (1)$$

If the above calculation results in an index of synergy significantly higher than 0, it can be concluded that a synergy exists to stabilize the performance variable and that the system functions according to the UCM hypothesis. Higher indices of synergy indicate stronger synergies³⁹.

2.2.4 Hierarchical Control of Movement

The hierarchical structure of human motor control has been shown to have a close relationship with redundancy. Hierarchical control states that task demands are distributed across varying levels of control within the hierarchy^{5,8,11,13,25,34,39-41,53}, which can be viewed as a means of progressively decreasing the number of variables manipulated by each higher-control level of a hierarchy, which results in alleviating the problem of redundancy.

As mentioned earlier, when two people work together, like in many daily tasks, CNS is facing even more degrees of freedom. The question is how these two CNSs manage to work with each other. Does inter-personal synergy exist? There has been a debate on the existence of motor synergies among two persons (i.e., inter-personal motor synergy (IPMS)). Gorniak and colleagues⁴¹ showed there seems to be a trade-off in existence of synergies at different levels of hierarchy, suggesting that when all levels of control are present, force-stabilizing synergies exist at the higher level of control compared to the lower level in a single-person task. However, Domkin

and colleagues⁵⁸ showed that in a two-arm pointing task motor synergies at different levels of control existed at the same time to stabilize the task performance. Due to this controversy, and limited studies on joint actions from this perspective, we would like to investigate at which level of control synergy exists. We aim to examine this through a two-finger force matching task performed by two people.

From the hierarchical point of view, this task consists of various levels of control: The highest level of control is the task level, where the combined contribution of co-workers leads to achieving the task goal. The mid-level (the inter-personal level) where the total task force is shared between each person's hand. The lowest level of control is the between-fingers (Intra-personal) level, where the total force produced by each hand is being shared across the index and middle fingers of individuals. These levels of hierarchical control refer to the ability of the movement system to be broken down into sets of subsystems that can be analyzed individually. In order to quantify motor synergy at each level we will use the negation of covariance between elements of the system at each level of hierarchy according to a method that was recently proposed²⁵. This method, known as hierarchical variability decomposition (HVD), has been used to quantify intra-personal motor output and motor coordination. Within the HVD model, motor performance is quantified as a mean-squared error of a particular motor task outcome, which mathematically can be decomposed into two aspects of the motor task: accuracy and precision. Within this framework, motor coordination is quantified as co-variations of multiple effectors of the system. In this study, we extended this framework to inter-personal activities to examine several control aspects that two CNS utilize to interact with each other.

Chapter 3 : How do task constraints affect co-working behavior?

3.1 Abstract

This study investigated the effect of task constraints on inter-personal interactions when two co-workers work together. Some previous studies have suggested that inter-personal interactions indicate the emergence of inter-personal synergies as the control strategy adopted in co-working actions. Inter-personal synergies refer to the interactions formed for the task-specific enhancement of motor performance in the combined motor outcomes of two or more co-workers. We hypothesized that inter-personal synergies are present in co-working actions even when a secondary task constraint is introduced. Co-workers performed tasks that required maintaining either solely a linear equilibrium (i.e. explicit task) or an implicit rotational equilibrium as well as the linear. The results indicated that co-workers interacted with each other synergistically to achieve the shared task goal. We also found that co-workers performed worse in the explicit task when the additional task constraint was introduced. More specifically, when they had to achieve rotational stability on top of linear stability, they adopted a synchronous strategy to accomplish the implicit task carefully, thus compromising the accomplishment of the explicit task. Our results suggest that the communication between co-workers through the task constraints dictates the control strategies that co-workers adopt and the specific task that they work toward accomplishing.

3.2 Introduction

Human-human interactions (HHI) are frequent in our daily life such as hand-shaking, lifting and carrying heavy objects with a friend, assisting a child riding a bicycle, and playing games. To ensure that two or more people can perform a task accurately and successfully, they

need to interact with each other appropriately. Proper interaction is formed based on the constraints imposed by the task and exchange of sensory feedback such as visual, haptic, and auditory feedback between co-workers. Over the past decade, there has been a growing interest in studying the underlying mechanism of HHI. The majority of these studies have used constrained visuomotor tasks^{3,4,18,21,27,38,42,59-62}, where co-workers were required to complete a shared motor task while facing a monitor providing the visual feedback of their combined motor outcome. These studies concluded that two people could perform the task better^{4,62,63} or as well as²¹ one person alone performing the same task. Moreover, the addition of haptic feedback to the visual feedback has been shown to improve performance compared to when only visual feedback is presented. Most of these studies focused on the role of sensory feedback exchanged between co-workers on their performance of the task. However, our understanding of the control strategies that co-workers adopt to perform a shared motor task under different task constraints is limited.

On the other hand, the inherent redundancy in the human motor control system (i.e., having more degrees of freedom (DOF) than necessary for performing the tasks) has been overlooked in the HHI studies. In single-person actions, the issue of redundancy has been addressed using the notion of synergies, defined as organization of the redundant set of effectors by the central nervous system (CNS) to work together in a way that ensures high stability in the task performance. In inter-personal actions, where two co-workers need to complete a shared task, the problem of motor redundancy becomes even more exaggerated due to the increased number of independent effectors within the system. Thus, the central nervous system (CNS) may adopt different motor control strategies in the contexts of inter-personal action as it deals with the increased motor redundancy. However, how co-workers utilize this redundancy to complete the shared task is not clear. Previous studies have suggested that we might be able to extend the notion of motor synergies to inter-

personal actions^{2,7,19,27,33,34}. However, in this case, in the absence of a central controller, non-centralized processes such as dynamical mechanisms emerging from the visual or haptic linkages between co-workers could be responsible for the formation of synergy-like inter-personal interactions. Masumoto and colleagues tested this hypothesis in a finger force production task where co-workers were asked to work together to produce forces such that sum of their finger forces matched a target while provided with the visual feedback of their combined force. They suggested that the negative correlation between co-workers' forces showed that they used a compensatory strategy to ensure high stability in completing the task, indicating the formation of inter-personal synergy. They suggested that the visual feedback of the combined motor outcome induced this compensatory strategy and synergistic interactions between co-workers. However, it is not known how much of the visual information (history of combined motor outcome vs. the current state) is essential for the formation of synergistic interaction between co-workers. Moreover, it is still unclear how the addition of haptic feedback and additional constraints imposed by the task affect inter-personal synergy.

In single-person actions, several studies suggested that the CNS can adapt to perform several tasks simultaneously. For example, grasping a cup of coffee requires the CNS to produce grasping forces to achieve “linear equilibrium”, and grasping torques to achieve “rotational equilibrium” of the cup of coffee. It has been posited that the CNS can simultaneously stabilize the total force and total moment by forming independently controlled force-stabilizing and moment-stabilizing synergies. This is in line with the principle of superposition originally introduced in robotics. In this study, we seek to investigate if that is also the case for inter-personal actions in a constant multi-finger force production task performed by co-workers.

Moreover, studies on the CNS's control strategies in single-person actions show that there is a close relationship between redundancy and the hierarchical structure of motor control^{5,40,64}. In this type of control, the task is distributed across different levels in a hierarchical manner decreasing the variables required to be tuned by the higher control levels which alleviates the problem of motor redundancy faced by the CNS. To quantify the hierarchical organization in a single-person action, hierarchical variability decomposition (HVD) method was developed in a multi-finger force production task²⁵. This model decomposes the variability in the motor system into mathematically independent components that quantify consistency, repeatability, and bias in task performance. HVD uses the covariance between effectors' outcomes to quantify synergy. In this study, we aim to extend this hierarchical framework to two-person actions to describe how inter-personal performance and control strategies change under different task constraints.

Our experimental paradigm allows us to examine the two CNSs' control strategies when two tasks impose constraints. In particular, co-workers need to collaborate to achieve stability of linear and/or rotational equilibrium in our customized experimental setting. We asked co-workers to perform an isometric force production task by pressing two force sensors that were mechanically fixed on a stationary frame with index and middle fingers. In another condition, an additional task constraint was introduced which implicitly required the subjects to produce constant balancing moment of finger forces on a seesaw frame that had a fulcrum between the two persons. Consistent with studies on single person actions, we expect that co-workers generate force-stabilizing synergies and maintain their performance even when the additional constraint is presented.

3.3 Methods

3.3.1 Participants

Forty¹ young adults, both females, and males, between the ages of 18-35 years old were recruited from the University of Maryland, College Park (UMD). All the participants were right-handed according to the Edinburgh Handedness Inventory. Participants were free of any upper extremity injuries, neurological disorders, and musculoskeletal problems. This procedure was approved by the Institutional Review Board (IRB) of UMD.

3.3.2 Equipment

Experiment apparatus consisted of two monitors on a table separated by a blocker (Figure 3.1**Error! Reference source not found.**a). Four 6-DOF force/torque sensors (Nano-17, ATI Industrial Automation, Apex, NC, USA) were used to record the index and middle finger forces of the two participants (4 fingers X 2 co-workers). The sensors were placed on a customized seesaw-lever structure (Figure 3.1**Error! Reference source not found.**b). This device was made using a 3D printer and was placed on the table in front of the participants. Signals from the force sensors were amplified and digitized at 1000 Hz with data acquisition hardware [National Instruments DAQ- card-6024E] using a custom software program created with LabVIEW [National Instruments Labview 2017].

¹ power analysis was performed using G*Power with an alpha level of 0.05 and power 0.85

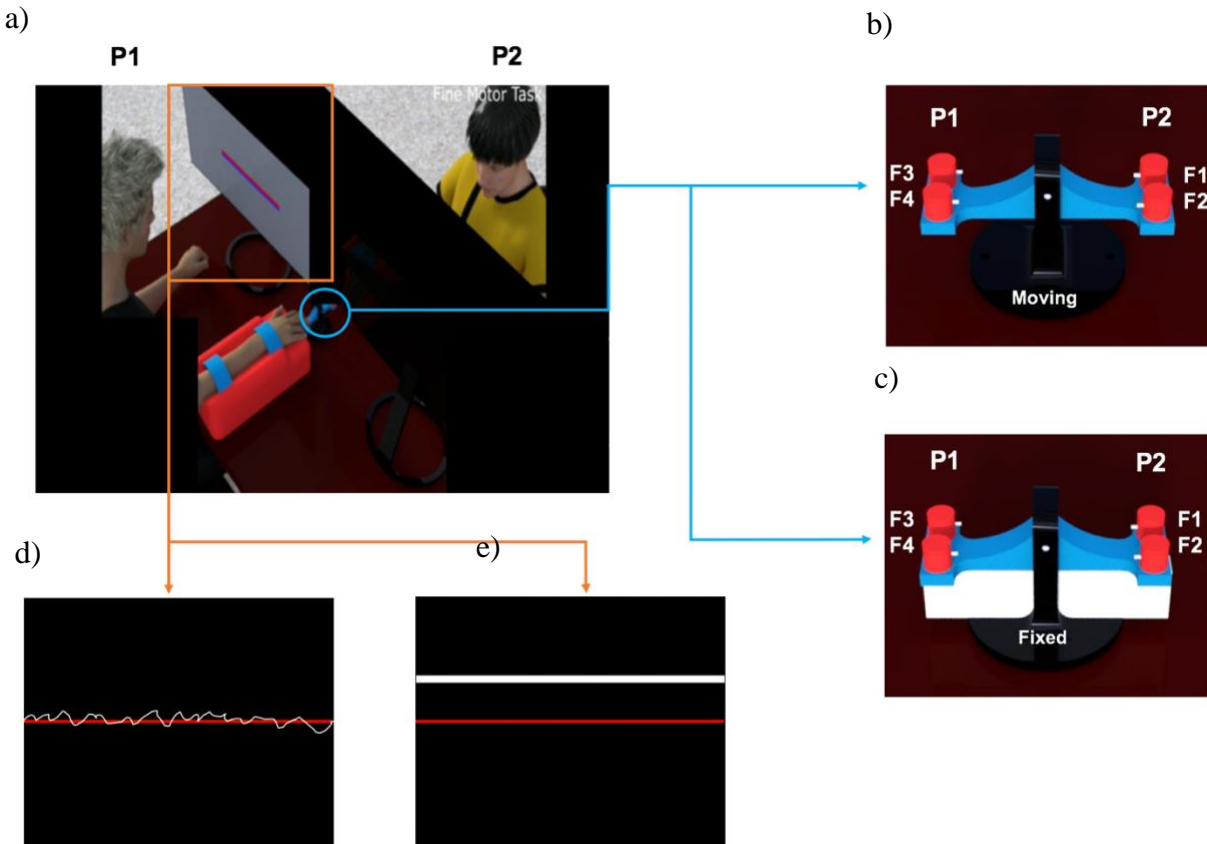


Figure 3.1. Experiment apparatus: a) Experimental setting. b) Customized seesaw with force sensors when it is freely moving about its axis of rotation. c) Customized seesaw with force sensors when it is mechanically fixed. d) Continuous visual feedback of the real-time force data, e) Instantaneous visual feedback of the real-time force data

3.3.3 Procedures

Participants sat on a chair facing a computer screen with the shoulder abducted 35° in the frontal plane and elbow flexed 45° in the sagittal plane such that the forearm is parallel to the frame. The forearm rested on the wrist-forearm brace (comprised of a piece of foam that was attached to a semi-circular plastic cylinder) fixed to a wooden panel (29.8*8.8*3.6 cm). Velcro straps were used to avoid forearm and wrist movements. Co-workers were asked to work together toward completing a target-tracking task. Subjects received visual feedback of the experimental task (i.e., constant target force line) and the real-time force line (i.e., the force they were producing)

on their monitor screens. Prior to the start of each trial, they received an auditory cue stating: “standing by”, which indicated that participants should rest their index and middle fingers of their right hand on the force sensors. In addition, an audio signal sounded at both the beginning and end of each 23-second trial. Participants were asked to start pressing on all of their force-sensors as soon as they hear the first audio signal sounded, to match the real-time force line to the target force line as soon as possible and maintain their force for the duration of the trial. The audio signal at the end of the 23-second trial indicated that the trial has ended and that participants should stop pressing on the force sensors. They repeated performing the same task for ten trials. Throughout the experiment, participants were asked to remain quiet and not communicate verbally.

This experiment contained four different conditions (Table 3.1), which were randomly assigned to co-workers. Each condition consisted of 10 trials of 23 seconds long, and 25 seconds of rest in between trials. For each trial, on their monitors, participants could see a red horizontal line that sat motionless midway up the screen. This line represented the experimental task, the target force of 10N for the first 13s of the trial and 20N for the rest of the trial (i.e., red target line). Along with the red target line, in the first 13 seconds of each trial, they received the visual feedback of their own (individual) force; this part of the trial is described as the “solo” part throughout this paper. This part was included for prescribing the approximate share of force that each participant contributed to the target force. Therefore, we could avoid any sort of burden on any of the partners and convey that the task was being shared between participants evenly. In the last 10 seconds of each trial, the sum of forces produced by two partners was displayed on the screen. This part of the trial is called the “co-working” part throughout this paper. It’s worth mentioning that participants were not aware of any of these parts; they just knew that they need to match their force to the target line.

Table 3.1. Different Conditions of Human-Human Interaction (HHXX) in Experiment I

Human-Human Interaction		Visual Feedback of real time force data	
		Continuous	Instantaneous
Haptic Feedback	Moving	Condition 1 (HHMC)	Condition 2 (HHMI)
	Fixed	Condition 3 (HHFC)	Condition 4 (HHFI)

Below, all four conditions will be explained in detail:

Condition 1. Moving seesaw with Continuous visual feedback of the real-time force data (HHMC):

In this condition, the seesaw was freely moving (Figure 3.1b) about its axis of rotation as participants pressed on the force sensors attached to it. Therefore, each person could feel his/her partner's force. On their monitors, along with the red target line, the force that participants produced in the solo and co-working parts were visualized in the form of a white curve (Figure 3.1d). This curve was continuously shown on the screen based on the pressure participants exerted on the force sensors. So, participants could see the whole course of the real-time force trajectory, including the past states as well as the current states. In this condition, participants

Condition 2. Fixed seesaw with Continuous visual feedback of real-time force data (HHFC):

In this condition, the seesaw was mechanically fixed (Figure 3.1c). Thus, participants could not feel their partner's force. The visual feedback that they received was the same as condition 1 (Figure 3.1d).

Condition 3. Moving seesaw with Instantaneous visual feedback of the real-time force data (HHMI):

In this condition, the seesaw was freely moving about its axis of rotation (Figure 3.1b). On their monitors, along with the red target line, the force that participants produced in the solo and coworking part were visualized in the form of a horizontal black line (Figure 3.1e). This line traveled vertically up and down the screen based on the amount of pressure participants exerted on the force sensors at each moment. Thus, participants could only see the force generated at the current time.

Condition 4. Fixed seesaw with Instantaneous visual feedback of real-time force data

(HHFI):

In this condition, the seesaw was mechanically fixed (Figure 3.1c), and the visual feedback that participants received was the same as condition 3.

3.4 Data Analysis

3.4.1 Hierarchical Variability Decomposition (HVD)

We quantified inter-personal motor performance as the overall mean-squared error (OMSE), the averaged squared deviation of the total force (i.e., the sum of individual person's forces combined) from the target force ($f_T = 20N$):

$$OMSE = \frac{1}{N} \sum_{i=1}^N \frac{1}{\tau} \int_{t=0}^{\tau} [f_T - y_i(t)]^2 dt \quad (1)$$

Where N is the number of trials, $y_i(t)$ is the total force at trial i , and τ is the duration of the trial. Note that from each 23-second trial, the 5-second window from 16 seconds to 21 seconds, where the total force produced was relatively constant and stable, was extracted for analysis in order to avoid the initial force stabilization at the beginning of each trial and premature cessation of force production at the end^{5,53}.

OMSE can be decomposed to three error components of performance variables: 1) The online error (i.e., online variance): defined as the variance within a trial, averaged over the trials. This value is a measure of consistency in task performance. 2) The offline error (i.e., offline variance), defined as the variance across trials. This variable identifies how well pairs repeated the task over multiple trials, and 3) the systematic error, defined as squared deviation between target force and the mean total force after averaging over all timesteps of all ten trials. This variable quantifies the bias in the task performance and how accurate pairs estimated and performed the task.

Using the hierarchical structure of variability (Figure 3.2), the online and offline errors can be further partitioned into the sum of individual person's force variances (i.e., $\text{Var}(P_1)$), plus between-person covariances (i.e., $\text{Cov}(P_1, P_2)$). We call this level of the hierarchy the inter-personal level, and we used online and offline covariances to quantify the interaction between co-workers. If they are positive, they indicate error amplification, while negative values indicate error compensation. A negation of covariance value is mathematically the same as the motor synergy quantified in previous studies⁶⁴⁻⁶⁷. In those studies, synergy is calculated within the uncontrolled manifold (UCM) framework³¹, as the difference between effector variance in the task-irrelevant space (UCM space), and the task-relevant space (Orthogonal space) that indicates the motor task error. UCM space specifies the CNS's ability in the utilization of the redundant degrees of freedom for task performance, while the orthogonal space variance identifies the motor task error. In the appendix, it was proved how these two methods are related to each other, and how the negation of covariance is the same as the index of synergy.

Finally, at the lowest level of the hierarchy shown in Figure 3.2, each person's variance is decomposed to the variance of their finger forces (i.e., index $\text{Var}(F_I)$ and middle $\text{Var}(F_M)$) and the

covariance between finger forces (i.e., $\text{Cov}(F_i, F_M)$). The covariance terms at this level represent the within-trial and trial-to-trial interactions of multiple fingers during force production; thus, they are used as a measure of multi-finger synergy associated with the finger force production task.

All the outcome variables of the HVD model (i.e., the 22 variables shown in Figure 3.2) will be defined for both experiments I and II within a custom program written in MATLAB software (Mathworks, Inc., MA, USA).

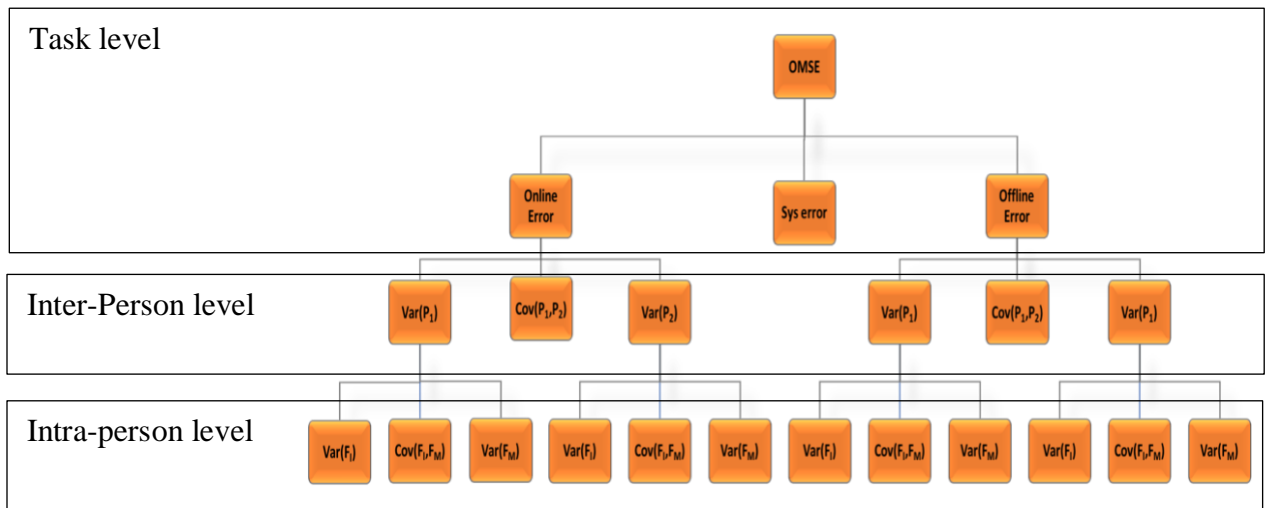


Figure 3.2. Hierarchical organization of dyadic performance in a redundant multi-finger force matching task

3.4.2 Statistics

For the statistical data analysis, a two-way repeated measure ANOVAs with factors Haptic Feedback with two levels (Moving Seesaw and Fixed Seesaw) and Visual Feedback with two levels (Continuous and Instantaneous) will be used to compare the outcomes of HVD model across different conditions at all levels. The level of statistical significance was set at $p=0.05$. We performed a Post-hoc test with Bonferroni correction in case of significant interaction to determine which factor caused the significant difference.

3.5 Result

3.5.1 Force trajectories

Figure 3.3 demonstrates force trajectories in a single trial for a representative subject in HHMC and HHFC conditions. HVD analysis was performed on force trajectories for all pairs (Figure 3.4).

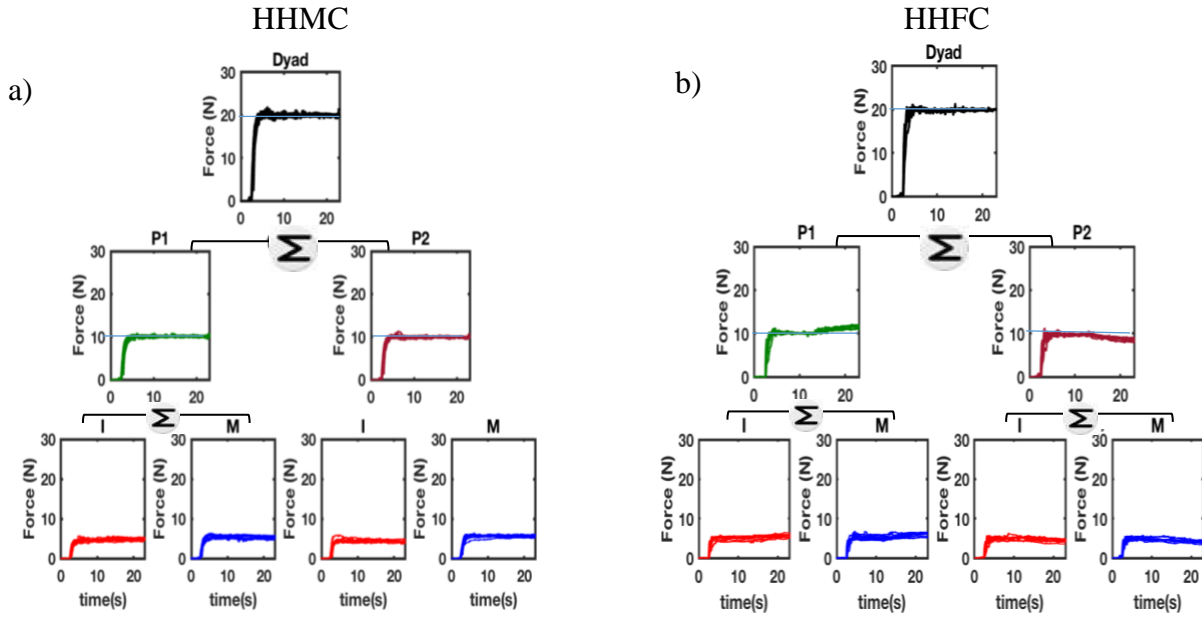


Figure 3.3. Force trajectories in a hierarchical manner for a representative pair in a) HHMC condition and b) HHFC condition. In both figures, bottom figure (intra-personal level) represents the forces recorded from individual index (I) and middle (M) fingers. The mid-level (inter-personal level) shows sum of index and middle finger forces produced by person one (P1) and person two (P2). Finally, the top level, task level, demonstrates sum of forces produced by two persons.

As our first aim, we were interested in expanding the developed HVD model for intra-personal activities to inter-personal actions and using this framework as a means for quantification of inter-personal motor performance and synergy. Figure 3.4 demonstrates this three-level hierarchy. At the top-level (i.e., task level) motor performance is quantified as the OMSE which is further decomposed into three error components that represent consistency (i.e., Online Variance), repeatability (i.e., Offline Variance), and bias (i.e., Systematic Error) in the

performance. At the mid-level (i.e., inter-personal level) Online and Offline Variances of each participant's force in addition to the Covariance between forces produced by individuals are shown. As mentioned previously, the Covariance term is a measure of the interactions between co-workers, and negative Covariance is the same as the index of synergy. Finally, at the bottom level (i.e., intra-personal level), Online and Offline Variances of each finger force in addition to the Covariance between forces produced by each finger are represented. Based on this hierarchy, we can examine aims two and three:

3.5.3 The role of task constraints in inter-personal motor performance and synergy

We intended to examine how task constraints affect inter-personal motor performance and synergy. Figure 3.4 summarizes the results according to HVD analysis. A two-way analysis of variance was conducted to examine the effect of manipulation of visual (i.e., Instantaneous vs. Continuous) and haptic feedback (i.e., Moving vs. Fixed) on inter-personal motor performance and synergy. At the task level of hierarchy, using an alpha level of 0.05, a main effect of haptic feedback on OMSE ($F(1,84) = 5.7, p = 0.02$), Online Variance ($F(1,84) = 10.14, p = 0.002$), and Offline Variance ($F(1,84) = 4.17, p = 0.044$) was observed. The results showed higher OMSE error, within and between trial variability for the Moving condition compared to the Fixed. However, no main effect of visual feedback, and no interaction *visual* \times *haptic* were observed. Moreover, the systematic error did not differ across different visual and haptic conditions. So contrary to our hypothesis, the results were not affected by the manipulation of visual feedback. In addition, the Fixed condition showed less error compared to Moving. From the HVD analysis on our data, we can conclude that higher OMSE in the Moving condition is mainly due to the higher within-trial variability (i.e., Online Variance) in this condition.

At the between-person level, between-person Online Covariance for the Moving condition was statistically greater than zero (for HHMI: $t(21)=7.38$, $p<10^{-6}$, HHMC: $t(21)=7.96$, $p<10^{-7}$) independent of the visual feedback presented to the pairs. This finding indicates the synchronous strategy dictated by the additional task constraint. However, it was statistically less than zero for the Fixed condition (for HHFI: $t(21)=-5.89$, $p<10^{-6}$, HHFC: $t(21)=-4.26$, $p<10^{-4}$) indicating the compensatory strategy between co-workers as expected. In addition, between-person offline covariance for HHMI condition was not statistically different from zero, but it was less than zero for HHMC ($t(21) = -3.5686$, $p=0.0018$), HHFI ($t(21)= -6.3571$, $p<10^{-4}$), and HHFC ($t(21)= -4.3847$, $p= 0.0003$) conditions. Comparing between-person online and offline covariances for the Fixed and Moving conditions, we found statistically significant differences between the two conditions (for online: $F(1,84)=125.8$, $p<10^{-16}$) and offline: $F(1,84) = 41.23$, $p<10^{-9}$). So, in the Fixed condition synergy exists at between-person level. However, for the moving condition, we found bad (wrong) synergy at between person level. Moreover, a main effect of haptic feedback on individuals' Online ($F(1,84) = 17.55$, $p<10^{-5}$) and Offline ($F(1,84) = 43.55$, $p<10^{-9}$) variances was found. Moving condition showed higher within and between trial variability at the individual's level compared to the Fixed condition. It is worth mentioning that no between-subject differences were found at this level.

At the within-person level, there were not any between-subject differences. A main effect of haptic on the online variance of index ($F(1,43)=19.62$, $p<10^{-6}$) and middle finger ($F(1,43)=11.77$, $p<0.001$) forces was found. They were higher in the fixed condition compared to moving. However, the offline variance of the index and middle fingers and online and offline covariances between fingers did not differ across different conditions. Between-finger online covariance for HHMI and HHMC conditions was significantly less than zero, indicating the

existence of intra-personal synergy at this level of control. However, this value was not significantly different from zero in HHFI and HHFC conditions. Offline covariance for all conditions was significantly less than zero indicating the existence of intra-personal synergy in offline control.



Figure 3.4. HVD analysis for different conditions of HHI experiment. The gray and pink bars show instantaneous condition, respectively.

3.6 Discussion

3.6.1 The role of task constraints in co-working behavior

Our experimental setting examined the effect of an additional task constraint on inter-personal motor performance by allowing the haptic feedback to be exchanged between co-workers. In the moving conditions, both visual and haptic feedback was present to subjects, while in the fixed conditions, only visual feedback of co-workers' combined motor outcome was accessible. Previous studies have suggested that haptically linked co-workers perform visuomotor tasks better or as well as either member alone^{18,21,43,47}. However, this improvement in performance might not be solely due to the haptic channel between two partners but because two people (rather than one person) are involved in the task. Our experimental setting examined the effect of haptic feedback and the task constraints imposed by it on inter-personal motor performance systematically as we have both moving (where both visual and haptic feedback is present to subjects) and fixed conditions (where only visual feedback is accessible). Our results showed that in both conditions, co-workers were able to perform the task successfully, even though they have not shared a common neural substrate. However, contrary to previous studies and our hypotheses, the exchange of force through the haptic channel between co-workers (through the seesaw-lever structure) did not seem to improve performance. In other words, co-workers perform worse when the seesaw was moving. HVD analysis allowed us to realize that the great source of this discrepancy was online variance. Looking at the decomposition of online variance to the lower level of control, we realized that it was mainly due to the inter- and intra-personal interaction strategies that people choose to adopt under different task constraints.

We found that visual coupling alone could induce synergistic interaction between partners in our task and haptic interaction was an impediment for that coupling; as it introduced another task constraint (e.g., stabilization of seesaw) to partners and created a conflict of interest with the task of target tracking. So, in the moving condition, we can say that the control of the tasks can be decoupled to control of two subtasks: the stabilizing sum of 1) forces ($F_{P1} + F_{P2}$), and 2) moments ($T_1 + T_2$) that independent controllers specify different control parameters to satisfy the tasks constraints. Figure 3.5 represents the number of elemental variables and constraints exist in Fixed as well as Moving condition.

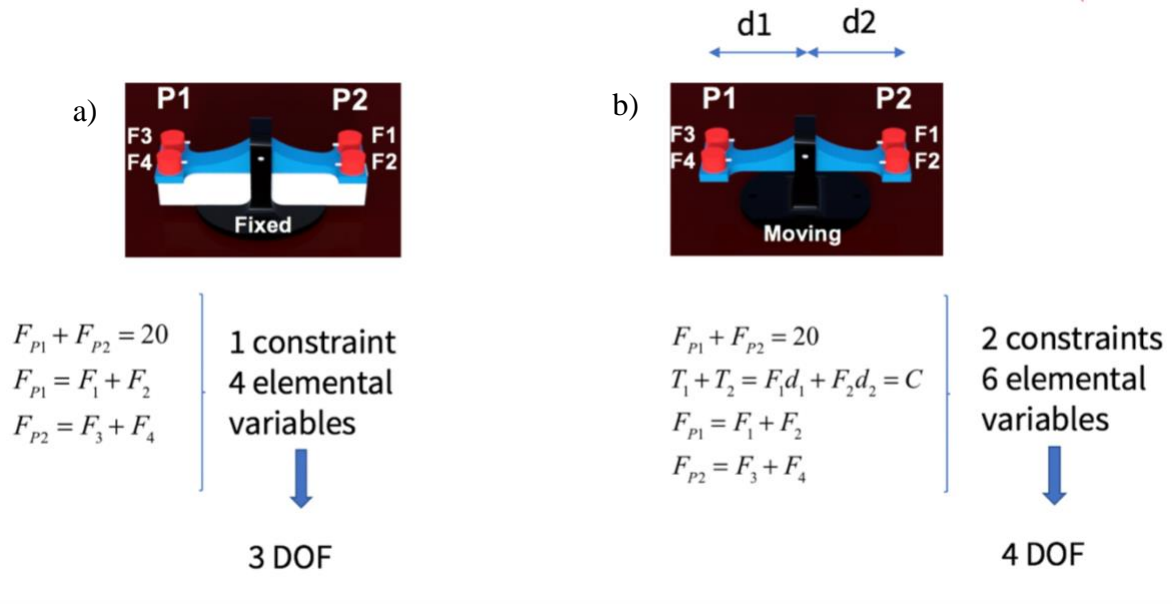


Figure 3.5. Task constraints and DOF in a) Fixed and b) Moving conditions

Looking at the online covariance, we see that the within-trial covariance between persons is positive in moving condition as opposed to fixed indicating that pairs adopted a synchronous strategy in moving condition but a compensatory strategy in the fixed one. Negative online covariance in the Fixed condition indicates moment-to-moment compensation between participants and it could be because now that the seesaw-lever is stabilized, each person is visually

"tracking" the other; in other words, we have compensatory tracking, and of course there will be a negative covariance between the error and the correction to it, which is the definition of negative feedback and in line with the previous studies^{5,17,34}. So, Fixed condition revealed the formation of moment-to-moment between-person synergy where they would create task-specific structural units to stabilize the task goal and adopt the same control strategy as intra-personal redundant actions²⁷. In the moving condition, contrary to our expectation, the haptic feedback found to impede the performance as partners were required to time their actions together^{2,61}. However, they were still able to complete the task successfully. Moreover, the coupling between co-workers reduced the redundancy as fewer effectors needed to be controlled due to the task constraints. In the Fixed condition, visual feedback is the dominant sensory information shared between partners and helps partners to interact with each other by focusing on the visual feedback of their combined action to perceive the consequences of their actions. However, in the moving condition, where both visual and haptic feedbacks are available, the fast-haptic feedback loops³³ from the mechanical linkage between partners (through seesaw-lever) overcome the visual feedback loops and cause co-workers to deviate from the task goal. In this case, they may interact synergistically toward completing another task, for example, stabilization of the seesaw-lever and form new synergies (e.g., moment stabilizing synergy)⁶⁸. Future studies can test this hypothesis by measuring the angle of the seesaw using the same experimental framework.

On the other hand, offline covariance for both conditions was negative (although more negative in fixed than moving condition), which indicates that over multiple repetitions, people tend to utilize different solutions to accomplish the task. In the moving condition, the existence of compensatory strategy in trial-to-trial but not in moment-to-moment suggests that error compensation at one level is not related to error compensation at the other level. This finding was

in line with research by Ranganathan and Newell's study in single person finger force production task. Moreover, results of online and offline covariance show that haptic feedback has a dual role in inter-personal coordination—removing the constraints on the degrees of freedom within trials by coupling partners and facilitating the utilization of redundancy between trials.

3.6.2 The role of task constraints in intra-personal synergy

First of all, manipulation of visual feedback did not affect intra-personal strategies for performing the task. However, haptic feedback did cause some differences: In the Fixed condition, we found zero between-finger online covariance indicating no synergy at this level. This suggests that CNS pairs DOF at this level and instead of sending individual signals to each finger at the between-finger level of control (so that each DOF acts individually), the CNS sends only one signal so that individual DOF activity is paired. This observation confirmed the results of Masumoto and colleagues⁵⁵ study, that symmetric strategy of the bimanual force production decreased the number of control variables; thus, participants were able to adopt a compensatory strategy with the total forces produced by the two participants. This finding is consistent with the optimal feedback control hypothesis⁵⁶, suggesting that the controller may not care about deviations in task dimensions that do not interfere with the task goal.

On the other hand, for the moving condition, we found negative between-finger online covariance indicating synergy at between-finger level. This finding would suggest that the CNS may simplify control at the lower levels of within-task control when performing a two-person task in the face of uncertainties coming from the mechanical constraints of the task. In addition, the observations of the existence of synergy at different levels of hierarchy (i.e., between-person or between-finger) in both conditions support the synergy trade-off theory previously mentioned^{39,69}. The finding suggests that CNS is only able to organize synergies on one level of control within a

given finger-force production task and the level at which synergy exists would depend on the task constraints. Finally, between-finger offline covariance for both moving and fixed conditions was negative, which suggests the utilization of redundancy over multiple repetitions in line with principal of minimal intervention and optimal feedback control theory⁵⁶.

3.7 Conclusion

In this study, we examined the role of task constraints on people's control strategies during HHI. We found that the additional task constraints (i.e., stability of linear and rotational equilibrium) deteriorates co-working performance. In this case, co-workers chose synchronous strategy to work in favor of accomplishing the rotational equilibrium task and not the explicit task linear stability as there were more DOF in the former task. We concluded that the mechanical constraints imposed by the task dictate the sort of control strategies (i.e., compensatory or synchronous) that people choose to interact with their co-worker.

Chapter 4 : Do we work together synergistically?

4.1 Abstract

Previous studies have provided evidence that independent brains work together synergistically to achieve their common goal if they share the visual information of their performance. However, it is not clear if live interaction with a human co-worker is a necessity for the formation of the synergistic interaction between the co-workers. Twenty-five co-workers completed two isometric finger force production experiments. In Experiment 1, co-workers isometrically produced finger forces such that combined force will match a target force, visually shown on a monitor in front of them. In Experiment 2, without participants' knowledge, each performed the same task with the playback of his/her co-worker's force trajectory previously recorded from Experiment 1. Comparison between the results of two experiments showed that co-workers achieved the same level of motor performance with similar control strategies, irrespective of working with a human or non-human co-worker. Further analysis showed that we can predict co-working behavior if we get people to work with a non-human co-worker that has similar statistical characteristics as a human. These findings suggest that humans processed their co-workers as disturbance when they worked together.

4.2 Introduction

People coordinate their actions with the actions of others as in shaking hands, having a conversation, passing and receiving utensils, transporting furniture, playing sports, dancing, etc. In these motor tasks, independent brains are required to “work together” in order to produce desired outcomes of combined motor system behaviors and achieve a common motor task goal. Many of

us have observed the enhancement through co-working in many everyday activities. Previous studies have also suggested that two persons can perform the task better^{18,27,62} than each person perform the same task alone. Does this performance improvement depend on the interaction with a human co-worker? Or can we get the same level of performance by working with a non-human co-worker? In other words, do we work collaboratively and create synergistic interaction with our partner? Or do we work independently, and the improvement in performance emerges as a result of co-workers reacting to the feedback they receive from each other and the environment? Despite the growing body of research in the realm of Human-Human Interaction (HHI), our understanding of the co-working behavior has remained shallow.

The mechanisms of interactions between multiple muscles, multiple fingers, multiple joint, and multiple body segments controlled by one central nervous system (CNS) have been extensively studied^{11,18,31,40,41,53,70-75} in the framework of intra-personal motor synergy⁶⁸. This theory has been proposed as a potential solution for the problem of motor redundancy (i.e., having redundant effectors for performing most tasks both at muscular and kinematic levels)¹³ in the human motor control system. For example, consider we ask a person to produce a constant force of 10N with index and middle fingers for multiple trials. In order for this person to successfully achieve this constant force, a person's fingers must work synergistically to impart the desired force. This fine tuning of motor effector control can be used to generate consistent task performance during a single trial (online control), or to produce the same performance, over multiple trials (offline control). When errors in performance are detected by the sensory system, synergistic motor effector actions can mitigate these errors by reducing the effect of erroneous motor actions through error compensations between effectors⁵³. In particular, when the system has more effectors than it strictly requires performing a given motor action, the interaction between

the effectors may exploit the redundant degrees of freedom found in the motor system in order to produce robust motor performance¹¹.

Some of the studies on the control strategies that two CNSs adopt in HHI have suggested the formation of inter-personal synergy between co-workers toward completing a shared task^{5,7,27,34}. In these studies, visual feedback of the combined motor outcome found to play a critical role in the formation of synergistic interactions between the co-workers. According to these studies, by looking at the visual feedback of their combined motor outcome, co-workers tried to compensate for any deviation from the task goal and took a compensatory strategy. However, it is not clear if they adapt and react to each other's behavior, or they react to the visual feedback they receive. In the former case, human co-workers form a two-way connection, where they work interactively. While, in the latter case, working with a non-human co-worker with a similar behavioral characteristic as a human co-worker can also cause the synergistic interaction properties; even though, in this case, there is a one-way connection between a human and non-human co-worker and only one can adapt and react to the feedback. Ganesh and Colleagues have provided evidence that physical interaction with a non-human co-worker (e.g., force playback from different subjects) cannot improve performance as well as interaction with a human co-worker¹⁸. They suggested that the two-way connection and in particular co-worker's reaction plays an essential role in co-working behavior.

So, we speculate that in our novel experimental paradigm, synergistic interaction arises as a two-way connection between co-workers. To test this assumption, we designed two isometric finger force production experiments: In Experiment 1, co-workers isometrically produced finger forces such that combined force will match a target force. In Experiment 2, without participants' conscious awareness, each performed the same task with the playback of his/her partner's force

trajectory previously recorded from Experiment 1. So, in the second experiment, we cut the two-way connection between co-workers to tease out any changes in participants' performance and control strategies. Previously developed hierarchical variability decomposition (HVD)²⁵ method was used to compare the results of experiment 1 and 2. In addition, thorough analyses in frequency domain were done to further identify the underlying mechanisms behind co-working behavior.

4.3 Methods

4.3.1 Participants

Forty² young adults, both females, and males, between the ages of 18-35 years old were recruited through undergraduate or graduate courses at the University of Maryland, College Park (UMD). All participants were right-handed according to the Edinburgh Handedness Inventory. Participants were free of any upper extremity injuries, neurological disorders, and musculoskeletal problems. This procedure was approved by the Institutional Review Board (IRB) of UMD.

4.3.2 Equipment

Experiment apparatus consisted of two monitors on a table separated by a blocker (Figure 4.1a). Four 6-DOF force/torque sensors (Nano-17, ATI Industrial Automation, Apex, NC, USA) were used to record the index and middle finger forces of the two participants (4 fingers X 2 co-workers). The sensors were placed on a customized seesaw-lever structure (**Error! Reference source not found.**Figure 4.1b) that was placed on the table in front of the participants. Signals from the force sensors were amplified and digitized at 1000 Hz with a 16-bit A/D board [PCI

² power analysis was performed using G*Power with an alpha level of 0.05 and power 0.85

6034E, National Instruments Corp] using a customized software program created with LabVIEW [LabVIEW 2017, National Instruments Corp.].

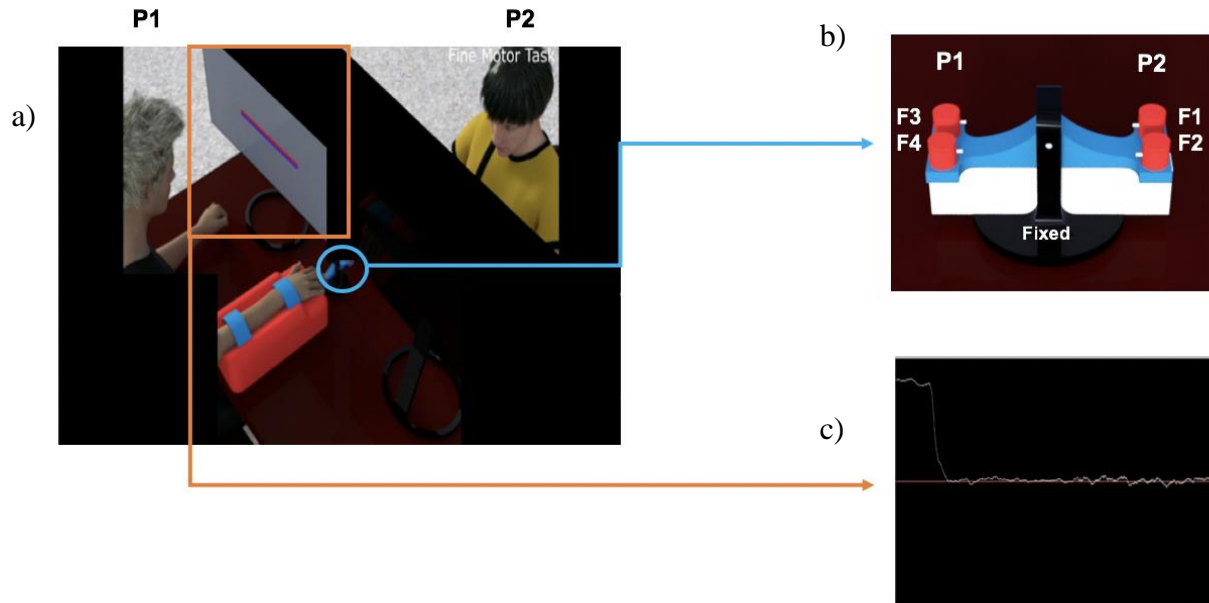


Figure 4.1. Experiment apparatus: a) Experimental setting. b) Customized seesaw with force sensors. c) Continuous visual feedback of the real-time force data

4.3.3 Procedures

Participants sat on a chair facing a computer screen with the shoulder abducted 35° in the frontal plane and elbow flexed 45° in the sagittal plane such that the forearm is parallel to the frame. The forearm rested on the wrist-forearm brace (comprised of a piece of foam that was attached to a semi-circular plastic cylinder) fixed to a wooden panel (29.8*8.8*3.6 cm). Velcro straps were used to avoid forearm and wrist movements. Two experiments were conducted: Experiment I) Human-Human interaction, and Experiment II) Human-Data interaction. In both experiments, they were asked to work together toward completing a target-tracking task. Subjects received visual feedback of the experimental task (i.e., constant target force line) and the real-time force line (i.e., the force they were producing) on their monitor screens (Figure 4.1c). Participants were asked to start pressing on all of their force-sensors as soon as they hear an audio cue, to match

the real-time force line to the target force line as soon as possible and maintain their force for the duration of the trial. They repeated performing the same task for 10 trials of 23 seconds long with 25 seconds of rest in between trials. For both experiments, participants were asked to remain quiet and not communicate verbally during the data collection.

Experiment I: Human-Human Interaction (HHI):

In this experiment, co-workers were asked to complete the mentioned target-tracking task. For each trial, on their monitors, participants could see a red horizontal line that sat motionless midway up the screen. This line represented the experimental task, the target force of 10N for the first 13s of the trial and 20N for the rest of the trial (i.e., red target line). Along with the red target line, in the first 13 seconds of each trial, they received the visual feedback of their own (individual) force; this part of the trial is described as the “solo” part throughout this paper. This part was included for prescribing the approximate share of force that each participant contributed to the target force. Therefore, we could avoid any sort of burden on any of the partners and convey that the task was being shared between participants evenly. In the last 10 seconds of each trial, the sum of forces produced by two partners was displayed on the screen. This part of the trial is called the “coworking” part throughout this paper. It’s worth mentioning that participants were not aware of any of these parts; they just knew that they need to match their force to the target line. For the sake of visual representation and for the force to continuously flow from the solo part to coworking part, we divided the latter part by 2, so participants would not notice any differences between solo and coworking parts. On their monitors, along with the red target line, the force that participants produced in the solo and coworking part were visualized in the form of a white curve (Figure 4.1c). This curve was continuously shown on the screen based on the pressure participants exerted on the force sensors. So, participants could see the whole course of the real-time force trajectory.

Experiment II: Human-Data Interaction (HDI):

This experiment consisted of two conditions in which participants worked with the playback of force data that their partner had produced previously in experiment I. The two conditions were randomly assigned to the participants. Table 4.1 demonstrates the conditions of this experiment.

Table 4.1. Different Conditions of Human-Data Interaction (HXD) in Experiment II

Experiment II: Human working with data		Coworking with data	Visual Feedback of real time force data
			Continuous
Haptic Feedback	Fixed	Solo part of the data	Condition 5 (HSD)
	Fixed	Coworking part of the data	Condition 6 (HCD)

Condition 1. Co-workers working with the playback of solo part of the data generated by their partner in experiment I (HSD): In this condition, in the solo part, like HHI experiment, participants received visual feedback of their individual force at the current time (F_1 for person 1 or F_2 for person 2 shown in **Error! Reference source not found.**) on their monitor. However, in the coworking part, each person worked with the playback of force produced by their partner in HHI experiment (Figure 4.2). Thus, without participants awareness, in the coworking part, on person 1's monitor, F_1+D_2 and on person 2's monitor F_2+D_1 was displayed, where D_1 and D_2 represents the playback of force data generated by person 1 and 2, respectively, between the 3-13s part of HHI experiment. The rationale behind taking this part of the data was that it often takes 2-

3 seconds for the participants to react to the auditory cue and reach to the target force. Therefore, we decided to remove the data produced in the reaction time of the task.

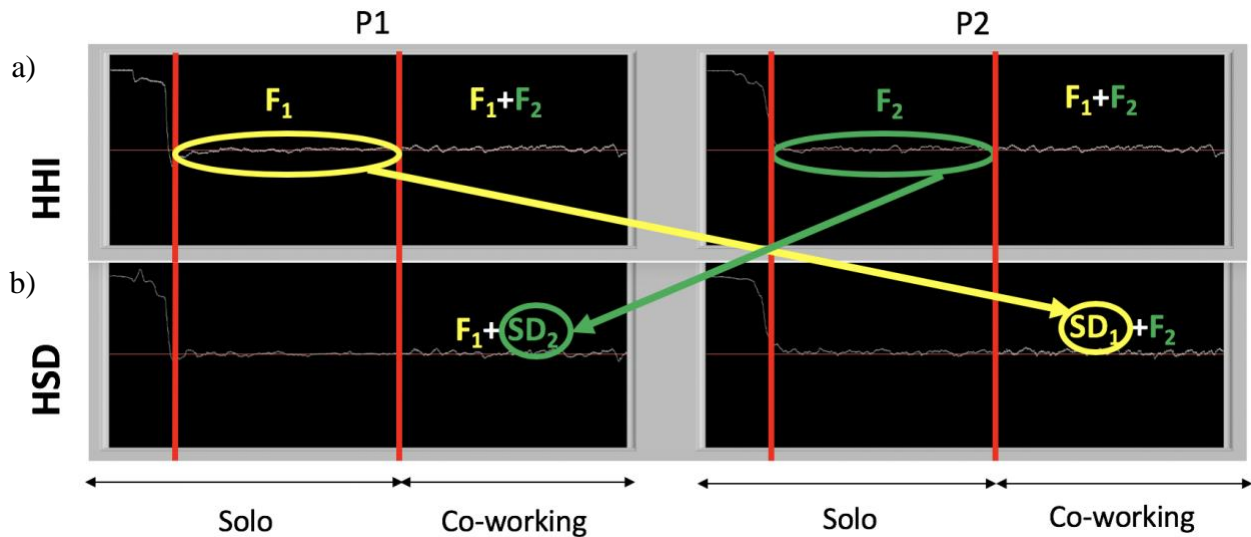


Figure 4.2. Demonstration of the visual feedback that participants receive in a) HHI experiment, and b) HSD condition of experiment II. Letter F denotes each participant's force at current time while letter SD represents the solo part of data recorded from HHI experiment.

Condition 2: Co-workers working with the playback of the coworking part of the data generated by their partner in experiment I (HCD):

In this condition, the solo part was again the same as before, however, in the coworking part, each person of a pair worked with playback of the coworking part of the trial (the 13-23 seconds of the trial) that had been recorded from their partner experiment I. Figure 4.3 represents this condition.

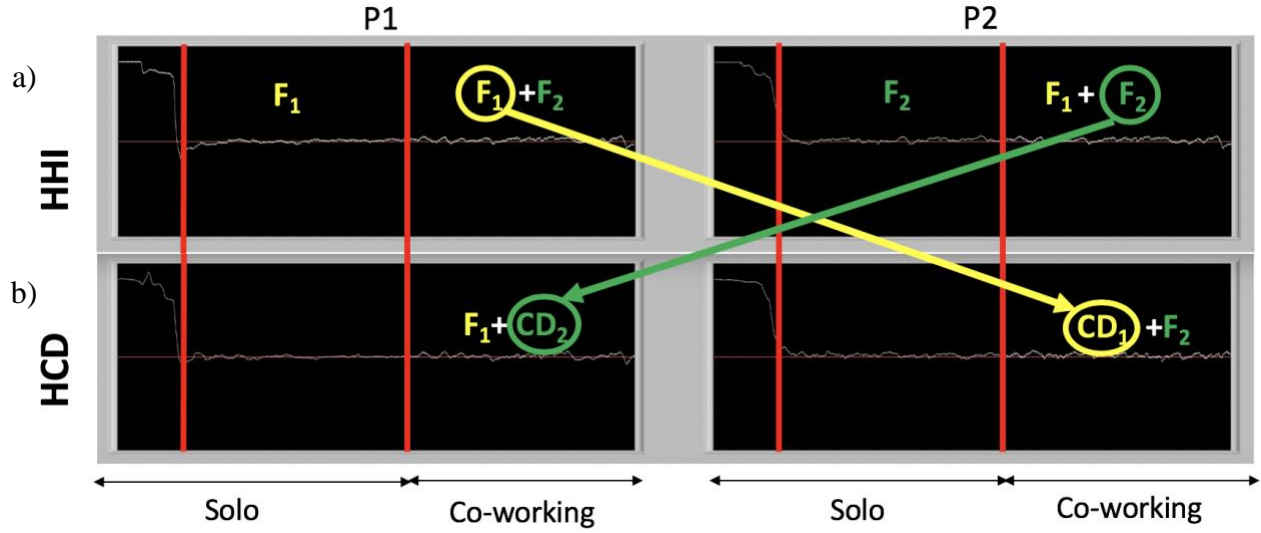


Figure 4.3. Demonstration of the visual feedback that participants receive in a) HHI experiment, and b) HCD condition of experiment II. Letter F denotes each participant's current force while letter CD represents the co-working part of data that was recorded from HHI experiment.

4.4 Data Analysis

4.4.1 Hierarchical Variability Decomposition (HVD)

We quantified inter-personal motor performance as the overall mean-squared error (OMSE), the averaged squared deviation of the total force (i.e., the sum of individual person's forces combined) from the target force ($f_T = 20N$):

$$OMSE = \frac{1}{N} \sum_{i=1}^N \frac{1}{\tau} \int_{t=0}^{\tau} [f_T - y_i(t)]^2 dt \quad (1)$$

Where N is the number of trials, $y_i(t)$ is the total force at trial i , and τ is the duration of the trial. Note that from each 23-second trial, the 5-second window from 16 seconds to 21 seconds, where the total force produced was relatively constant and stable, was extracted for analysis in order to avoid the initial force stabilization at the beginning of each trial and premature cessation of force production at the end^{5,53}.

OMSE can be decomposed to three error components of performance variables: 1) The online error (i.e., online variance): defined as the variance within a trial, averaged over the trials. This value is a measure of consistency in task performance. 2) The offline error (i.e., offline variance), defined as the variance across trials. This variable identifies how well pairs repeated the task over multiple trials, and 3) the systematic error, defined as squared deviation between target force and the mean total force after averaging over all timesteps of all ten trials. This variable quantifies the bias in the task performance and how accurate pairs estimated and performed the task.

Using the hierarchical structure of variability (Figure 4.4), the online and offline errors can be further partitioned into the sum of individual person's force variances (i.e., $\text{Var}(P_1)$), plus between-person covariances (i.e., $\text{Cov}(P_1, P_2)$). We call this level of the hierarchy the inter-personal level, and we used online and offline covariances to quantify the interaction between co-workers. If they are positive, they indicate error amplification, while negative values indicate error compensation. A negation of covariance value is mathematically the same as the motor synergy quantified in previous studies^{64–67}. In those studies, synergy is calculated within the uncontrolled manifold (UCM) framework³¹, as the difference between effector variance in the task-irrelevant space (UCM space), and the task-relevant space (Orthogonal space) that indicates the motor task error. UCM space specifies the CNS's ability in the utilization of the redundant degrees of freedom for task performance, while the orthogonal space variance identifies the motor task error. In the appendix, it was proved how these two methods are related to each other, and how the negation of covariance is the same as the index of synergy.

Finally, at the lowest level of the hierarchy shown in Figure 4.4, each person's variance is decomposed to the variance of their finger forces (i.e., index $\text{Var}(F_I)$ and middle $\text{Var}(F_M)$) and the

covariance between finger forces (i.e., $Cov(F_i, F_M)$). The covariance terms at this level represent the within-trial and trial-to-trial interactions of multiple fingers during force production; thus, they are used as a measure of multi-finger synergy associated with the finger force production task.

All the outcome variables of the HVD model (i.e., the 22 variables shown in Figure 4.4) will be defined for both experiments I and II within a custom program written in MATLAB software (Mathworks, Inc., MA, USA).

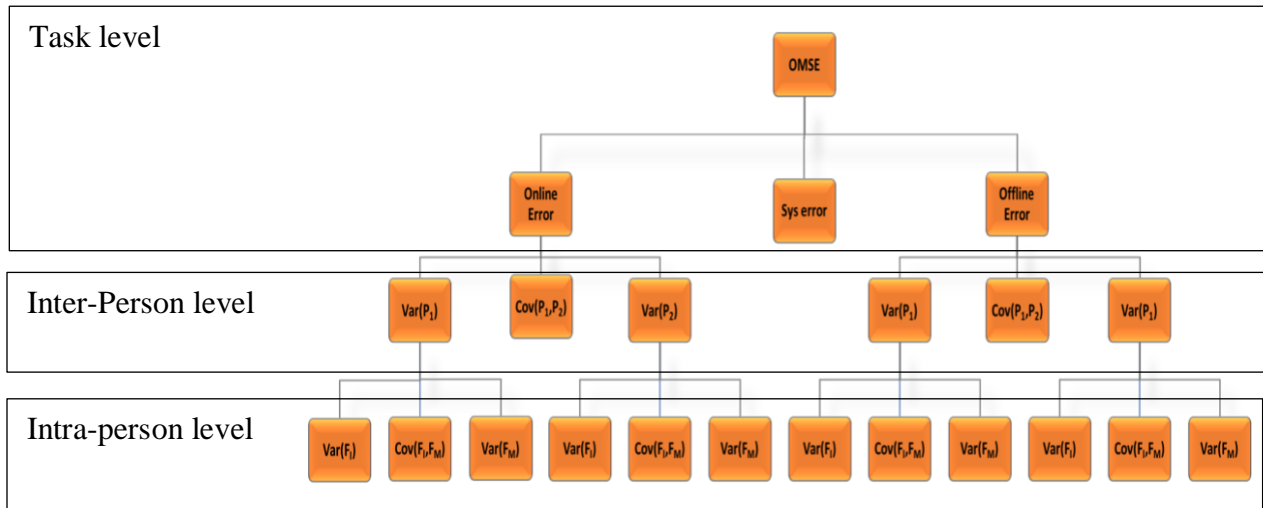


Figure 4.4. Hierarchical organization of dyadic performance in a redundant multi-finger force matching task

The above-mentioned hierarchy was created for Human working with a human co-worker and working with non-human co-worker, in other words it was created for HHI, HSD, and HCD conditions.

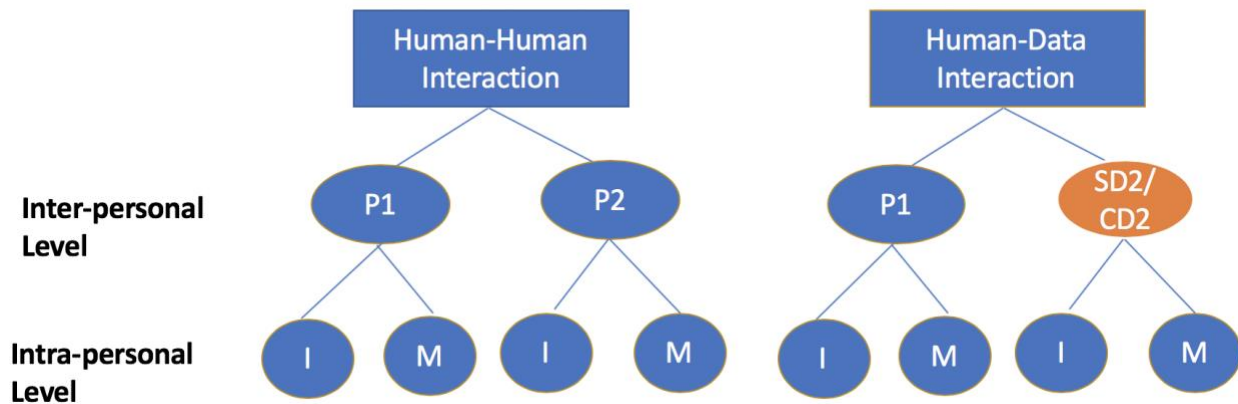


Figure 4.5. Hierarchical structure for human working with a) human co-worker, and b) non-human co-worker (working with solo part (SD2) or co-working part (CD2) of their partner's data)

4.4.2 Statistics

For the statistical data analysis, a one-way repeated measure ANOVA with Bonferroni adjustment was performed to determine if OMSE and synergy among HHI, HSD, and HCD conditions were significantly different. The level of statistical significance was set at $p=0.05$ for this case as well.

4.5 Result

4.5.5 Characterization of Inter-personal Motor Synergy

Figure 4.6 compares inter-personal motor performance and synergy for the HHI condition to HSD and HCD conditions. This graph is drawn for “person one” coworking with “person two” in HHI condition and the playback of data recorded from “person two” in HSD and HCD conditions. The same graph can be drawn for person two in collaboration with person one and their data. Remember that the selection of person one and person two was arbitrary, and there was not any statistical difference between them. One-way analysis of variance was conducted to compare mean OMSE, Online and Offline Variances, and systematic error of HHI, HSD, and HCD

conditions. Using an alpha level of 0.05, this test showed a significant difference in Offline Variance ($F(2,63) = 0.02$) at the task level. However, this test did not detect any statistical differences in OMSE, Online Variance, and Systematic error between these conditions. Post hoc Tukey HSD tests with Bonferroni adjustment indicated that Offline Variance was higher in HCD condition than HHI condition. As all task-level variables except for offline variance were not different from each other, the greater between trial variability in HCD condition can indicate that participants used different finger-force sharing pattern across trials to better work with their partner's trajectory playback. Therefore, they could create the same level of performance as if the two co-workers were interacting with each other. However, there was no difference in Offline Variance between HHI vs. HSD and HSD vs. HCD.

At the between-person level of the hierarchy shown in Figure 4.6, one-way analysis of variance showed significant differences in individuals' Offline Variance ($F(2,63) < 0.0003$), between-person Online covariance ($F(2,63) = 0.001$), and between-person Offline Covariance ($F(2,66) < 0.001$). Post hoc Tukey HSD tests with Bonferroni adjustment indicated that HSD had significantly less individuals' Offline Variance than HHI ($t = -3.974, p = 0.0005$) and HCD ($t = -3.231, p = 0.006$), indicating human working with solo part of their partner's data would create less variability across multiple repetitions. Post hoc Tukey HSD tests with Bonferroni adjustment indicated that HSD vs. HCD ($t = 3.316, p = 0.00456$) and HSD vs. HHI ($t = 3.313, p = 0.00460$) differed significantly in the Online Covariance, while, HCD and HHI conditions were not found to be statistically different from each other. In addition, t-test was run to see if covariance elements were significantly different from zero. According to this test, Online Covariance in HHI ($t(21) = -4.2, p < 0.0001$) and HCD ($t(21) = -4.5, p < 0.0001$) conditions found to be statistically less than zero, indicating compensatory strategy between co-workers but it did not differ from zero for HSD

condition, indicating that the two co-workers worked independently of each other. In addition, post hoc Tukey HSD tests with Bonferroni adjustment showed that between-person Offline Covariance in HSD was smaller than HHI ($t= 3.888, p=0.007$) and HCD ($t= 3.307, p=0.004$). We also ran t-test to see if covariance elements are significantly different from zero or not: for all HHI ($t(21) = -4.37, p= 0.0003$), HSD ($t(21) = -2.84, p<0.0099$), HCD ($t(21) = -4.49, p= 0.0002$), offline covariance was found to be statistically less than zero, indicating compensatory strategy for all the conditions. At within-person level, one-way analysis of variance showed a significant difference only in between-finger Online Covariance ($F(2,63) = 0.04$). Post hoc Tukey HSD tests with Bonferroni adjustment showed that between-finger Offline Covariance for HSD vs. HCD was significantly different ($t= -2.5, p=0.044$). So, synergistic interactions were observed in HHI between two co-workers and HCD condition between a human and co-working data playback.



Figure 4.6. Comparing HHI with HSD and HCD conditions

4.6 Discussion

4.6.1 Characterization of the co-working behavior

Surprisingly, we found that in all the cases, whether two humans are co-working (i.e., HHI) or playback of a recorded trajectory of human is one of the co-workers (HSD and HCD conditions), participants perform the task at the same level. In HHI condition, we have a two-way connection between partners where they receive visual feedback of their combined performance and try to react in a way that best fulfills the task goals. But HSD and HCD conditions present a one-way connection where a human subject can respond to errors while the partner (which is the playback) cannot respond. So, intuitively and according to previous studies^{18,35}, the absence of partner reaction should deteriorate performance. Contradictorily, looking at the highest level, task level, of the HVD model we can see that there was not any difference in task error (OMSE), within-trial variability (Online Variance) and estimation of the task goal (systematic error) between the three conditions. This interesting finding suggests that people processed their partner as disturbance. One potential reason for the discrepancy of our result with previous studies could be the existence of physical interaction between co-workers in those studies that found to be important for enhancing inter-personal performance^{18,21,35,43}.

More surprisingly were the differences we found between HSD and HCD condition at the between-person level of the HVD model. In the HSD and HCD condition, it's like people are responding to visual disturbances which are the playback of different parts of the data that was recorded from their partner in HHI condition. In HSD condition, people were set to work with a data that have never worked with or shared any information with, while in HCD condition they were working with the data that have previously worked with and shared visual information with. We found that Online Covariance between person and data in HCD condition was less than zero

(i.e., compensatory strategy) and it did not differ from HHI condition. In other words, people respond to this disturbance in the same way as if there is a third person that they are interacting with like HHI experiment. However, in line with our hypothesis, Online Covariance did not differ from zero in HSD condition indicating that the person works independently from the solo part of the data. It was surprising that we found the one-way connection between human and data (HSD vs. HCD) to differ from each other and it indicated that coworking part of the data has specific characteristics that are not present in solo part. This finding suggests that the perceived origin of forces can affect the way in which a person behaves³⁴.

For Offline Covariance, the same results were observed except that the covariance term in all the cases was less than zero even for HSD condition, indicating that over multiple repetitions people learn to adapt to the disturbance and try minimizing the deviation from the task goal. It is worth mentioning that as we expected variability of solo part of the data was smaller than coworking part and that's because in the coworking part two sources of noises (two people) are present which increases the uncertainty and variability. So, as the between-trial variability of individual's person and data forces for the solo part is smaller than co-working part, there was no need for co-actors to compensate for the error in HSD condition. But higher force variability in HCD condition required participants to compensate for each other's error. But this was not seen in online control. We did not find any differences in the individual's within-trial variability. Do these findings imply that we have multiple mechanisms in the system? In order to address this question and understand the differences between HSD and HCD conditions, spectral analysis was performed that will be explained thoroughly in the next section **Error! Reference source not found.**

4.6.1 Spectral Analysis

We performed closed-loop system identification of two-person performing a task using visual sensory perturbation. Studies of inter-personal actions that involve sensory feedback for ongoing corrections (i.e., closed-loop feedback system) have attempted to determine the underlying neural mechanism behind the interaction of two people using some performance measures such as task error. In order to better identify these mechanisms in a systematic way, we aimed at cutting the interaction between co-workers (shown to present in HHI (Figure 4.7a)) by designing experiment II (Figure 4.7b) to identify this interaction better. In this experiment, without participants' awareness, they were set to work with visual disturbances. In this case, we do not have a closed-loop feedback system anymore as the two-way connection between partners is cut, and we have only a one-way connection, we call this open-loop condition.

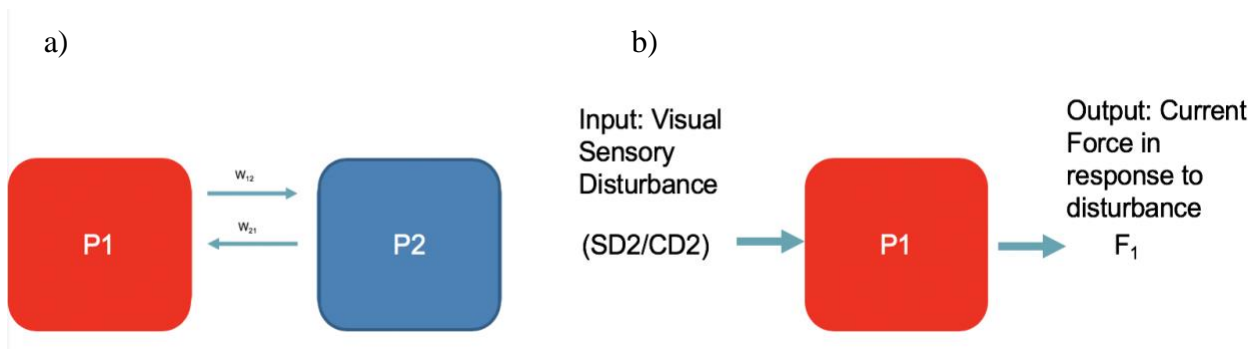


Figure 4.7. a) two-way connection between co-workers in HHI b) one-way connection between person and data (input-output mapping between visual sensory disturbances and force of the person in response to the disturbance), the same mapping can be formed for P2.

We assume that in experiment II, we have a single input single output linear time-invariant system with two sorts of visual disturbances (i.e., SD2/CD2: playback of data recorded from different parts of HHI condition) as input and force of people in response to those perturbations as output. The underlying assumption of this linear mapping is to have a linear time-invariant system. The most reasonable part of the data for this assumption was the part of data that the force signals

were stationary (i.e., 6-11s for the solo part and 16-21s for the coworking part); this part was also used in the HVD analysis explained in previous section.

As the second step, we would like to tease out any discrepancies between the two open loop conditions. These differences could be due to three sources: 1) the differences in statistical properties of the two inputs (disturbances), which can be done by comparing the PSDs of inputs, 2) intrinsic variability (i.e., variability that is not due to the input) of the system under different disturbances, which can be done by comparing the conditional power spectral density, or 3) the differences in frequency response functions (FRF). In the following paragraph we define how each of these parameters were calculated:

For any two signals $x(t)$ and $z(t)$, the power spectral densities (PSDs) $P_{xx}(f)$ and $P_{zz}(f)$ and cross-spectral density $P_{xz}(f)$, where f is frequency, were computed using Welch's method⁷⁶ with 5-s Hanning windows and 50% overlap for each trial and averaged across the 10 trials for the given condition. And the conditional spectral density⁷⁶ was computed using $P_{xx,z} = P_{xx}(f) - C_{xz}(f) P_{xx}(f)$ which is the portion of PSD of x not related to z . In this equation, $C_{xz}(f) = \frac{|P_{xz}(f)|^2}{P_{xx}(f)P_{zz}(f)}$ is the coherence between the two signals. In our case, z is the input (SD2/CD2) and x is the output signal (F1). In addition, the closed-loop FRF from $z(t)$ to $x(t)$ is $H_{zx}(f) = p_{zx}(f)/p_{xx}(f)$. Gain is the absolute value of $H_{zx}(f)$ and phase is the argument of $H_{zx}(f)$, converted to degrees. A positive phase indicates that $z(t)$ was phase advanced relative to $x(t)$.

Now we can examine each of the three cases one by one:

1. Differences in statistical properties of inputs: For HSD condition, the input for P1 was solo part of the data (SD2) and for HCD condition, it was co-working part of the data (CD2) each of which was recorded form HHI experiment. The same thing was calculated for P2.

Figure 4.8 shows the comparison between the PSDs of these two inputs.

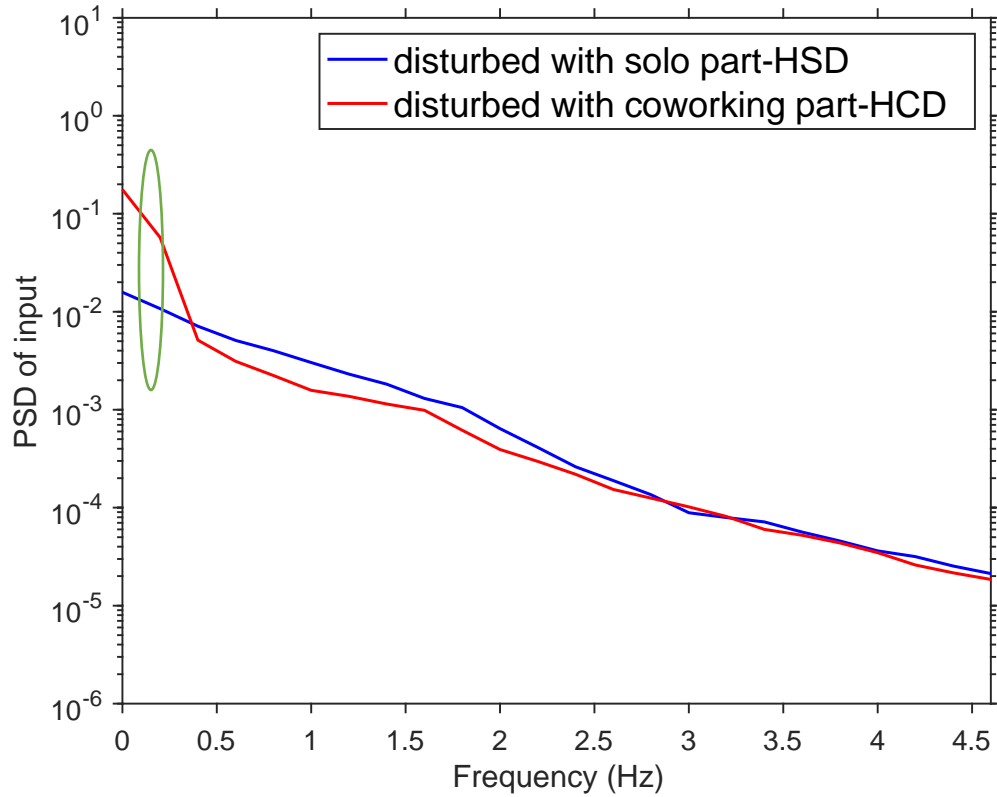


Figure 4.8. Comparing the PSDs of two different inputs. Input in HSD condition was solo part of data recorded from HHI (SD2) and HCD condition it was co-working part of data recorded from HHI (CD2).

T-test with false discovery rate (FDR) adjustment resulted in statistical differences between PSDs of the two inputs at 0-0.2 Hz. More specifically, the PSD in HCD condition was larger than the HSD condition at low frequencies.

2. Intrinsic variability of the system. The conditioned PSDs for the outputs (F1), which was the power of F1 given the input were calculated for HSD and HCD conditions. Figure 4.9 shows the results of this comparison

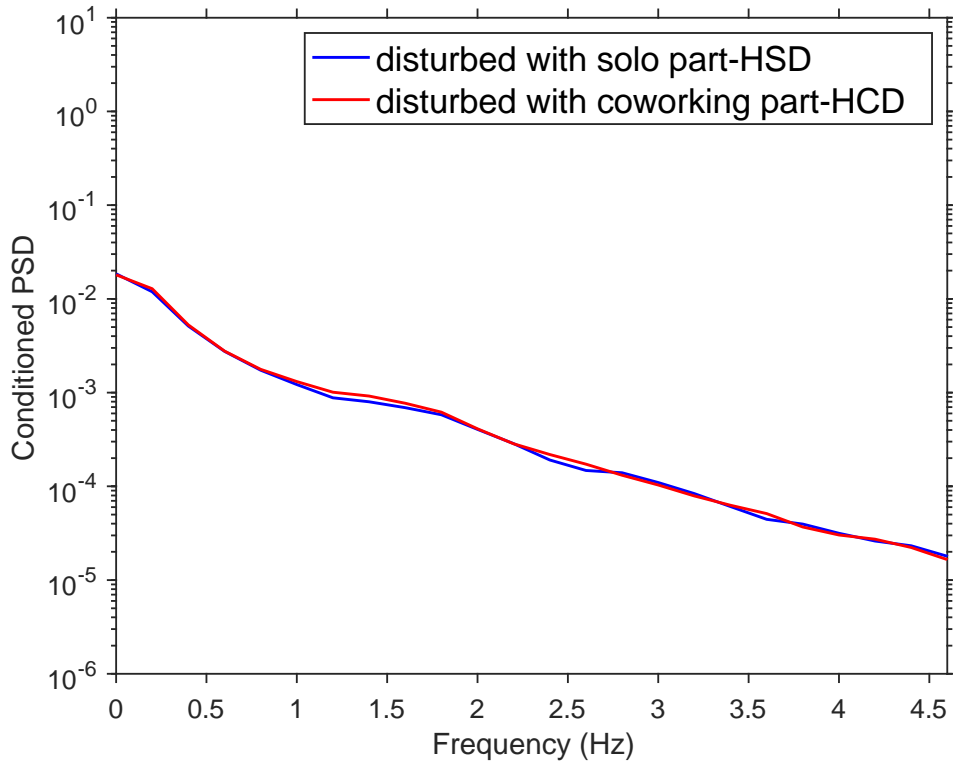


Figure 4.9. comparing the conditioned PSD for HSD and HCD conditions

T-test with false discovery rate (FDR) adjustment did not show any statistical differences between the conditioned PSDs in two conditions, indicating that intrinsic variability, or more specifically the mechanism of the system did not change by changing the inputs.

3. Differences in FRF: FRF was calculated in HSD and HCD conditions. The gain and phase of the two FRFs are shown in Figure 4.10

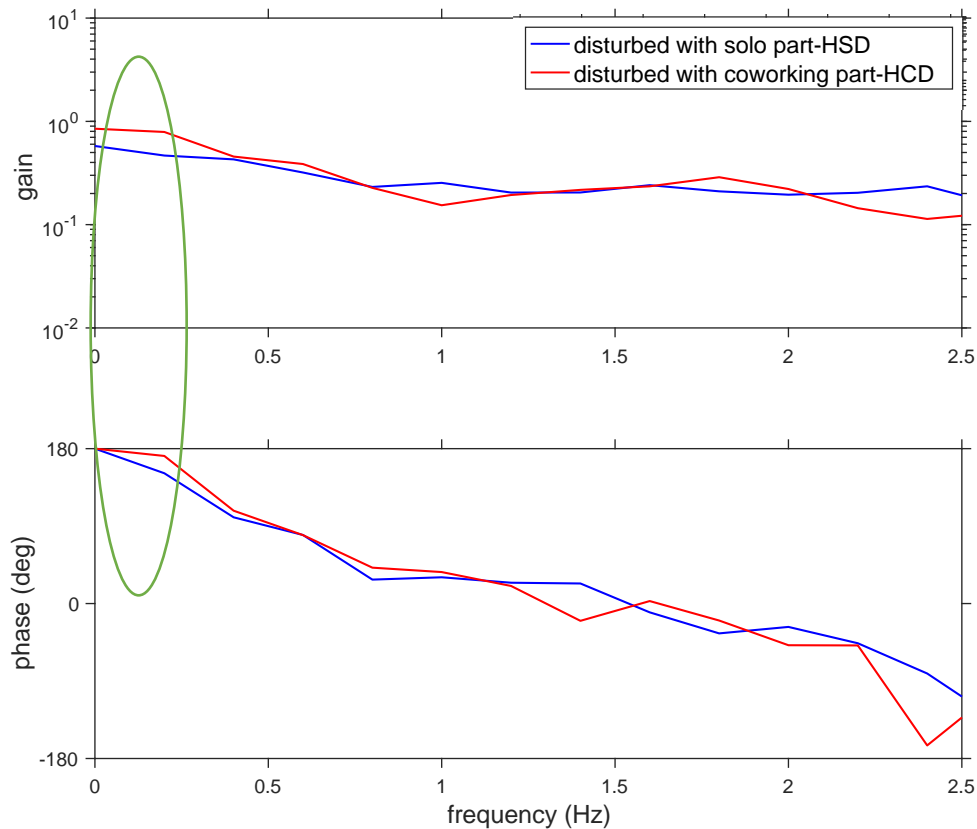


Figure 4.10. The gain and phase of FRF in HSD and HCD conditions

Hotelling T^2 with FDR adjustment indicated that FRF for the two disturbances was significantly different from zero at frequencies [0-2.4 Hz]. Moreover, the two FRFs were significantly different from each other only at frequencies between 0-0.2 Hz.

Therefore, the differences between HSD and HCD conditions go back to the differences in the statistical properties (distribution of power across frequency) of the two disturbances at low frequencies. We found that the gain of FRF in the HCD condition was higher than HSD. This result represents that there is a source of non-linearity in the system. However, this non-linearity is not due to the presence of additive noise as we checked that through the comparison between the conditioned PSDs. This non-linearity is coming from the gain of response being dependent on the amplitude of the input. So, there is not one unique FRF explaining the mapping between input and

output. Therefore, the estimated FRF here depends on the input that we used. As larger input (HCD) resulted in larger gain, we can say that people behave more aggressively to larger inputs. However, this only happens at low frequencies. At high frequencies, the system responds to both disturbances in the same way.

For the next step, we wanted to confirm that playback of trajectory as the second co-worker is sufficient for generating co-working performance as we concluded from the HVD analysis at task level. In other words, we tested if we can predict the closed-loop behavior from any of the two open-loop cases. We wanted to identify the PSD of force in the closed-loop (e.g., when two people are working together), using the conditioned PSDs and FRFs from open loop conditions using the following formula (the proof is provided in the appendix):

$$PSD \text{ of } F_1 = \frac{H_1 P_{N_2 N_2} + P_{N_1 N_1}}{(1 - H_1 H_2)}$$

Where $P_{N_2 N_2}$ and $P_{N_1 N_1}$ are conditioned PSDs for person two and one, respectively. And, H_1 and H_2 are frequency response functions for person one and two defined for each of the open-loop conditions.

Therefore, three PSDs were calculated: 1) PSD of F1 from HHI, 2) PSD of F1 predicted from HSD, and 3) PSD of F1 predicted from HCD condition. Figure 4.11 shows the three mentioned PSDs.

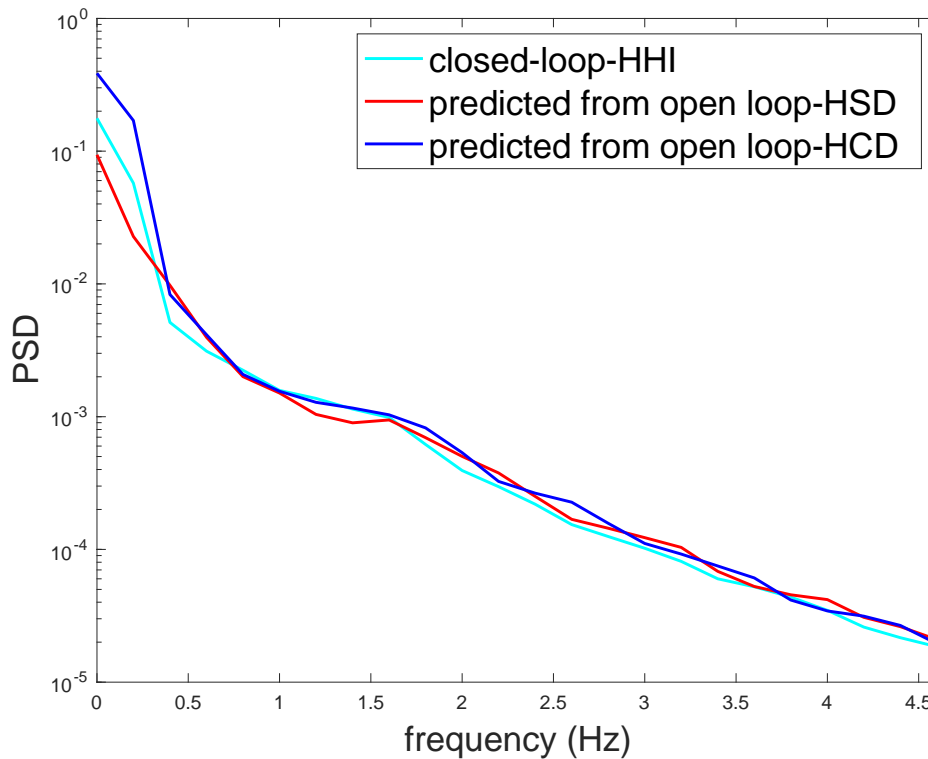


Figure 4.11. Predicting co-working behavior from open-loop conditions

T-test with FDR adjustment did not result in any significant differences between the PSD of individual's force in closed-loop condition and HCD. However, the PSDs in closed-loop condition vs. HSD and also PSDs in HSD vs. HCD conditions were significantly different at 0.2 Hz. So, we could predict the closed-loop PSD from HCD condition. These findings indicate that if we match the spectral density of the input in open-loop with the closed-loop, we can predict the closed-loop behavior from this open-loop condition. This finding confirms our claim from HVD analysis that no matter people are working with disturbances or actual human, they behave in the same way. However, the origin of this source of disturbance matters in the strategies that people choose, as we saw the differences in HSD and HCD conditions. However, in these experiments, we were dealing with a quasi-static task, and validity of these interpretations should be tested in dynamic and more complicated task.

4.7 Conclusion

We observed that co-workers achieved the same level of performance, irrespective of working with a human or non-human co-worker. In addition, playback of a recorded trajectory of human movement as a second co-worker appeared to be sufficient to generate co-working performance. Moreover, people working with a non-human co-worker tend to adopt similar strategies as co-working if the non-human co-worker has similar statistical characteristics as human co-worker. These findings suggest that in quasi-static tasks co-workers do not work synergistically to achieve better performance, but one processed another as disturbance when they work together

Chapter 5 : A feedback control model with Bayesian multisensory integration that simulates multi-finger synergy during constant finger force production

5.1 Abstract

One of the main questions in human motor control is how the central nervous system (CNS) uses the inherently noisy and delayed sensory feedback, to control its redundant effectors for performing the desired movement. In the present paper, we are seeking the answer to two main questions: First, to address how CNS integrates noisy, delayed multi-sensory information to coordinate the movement of its redundant motor elements. Second, to address how the absence of one sensory modality (tactile feedback in our case) affects the CNS control strategy. To do that, we proposed a feedback control model that simulates experimental data previously collected from participants performing constant finger force production task with and without tactile feedback, manipulated through the injection of anesthesia in fingers. This model could reproduce the experimental observations from this task faithfully, especially the synergistic interaction between fingers when tactile sensory feedback is present versus when it is absent. In-depth analysis of the model indicated that the removal of tactile feedback weakens synergistic interactions between fingers by increasing the sensory transduction delays and uncertainty in sensory measurements. In addition, short-latency feedback described in previous studies found not to be sufficient for reproducing synergistic interaction between fingers after removal of tactile feedback.

5.2 Introduction

Experimental descriptions of human movement have revealed a variety of possible mechanisms responsible for neural control of movement, which makes it challenging to comprehend how the complete system might work. Understanding the control mechanism of

human behavior through modeling approach can contribute to the identification of the systemic mechanisms observed in experimental studies; suggest testable hypotheses, and finally aid in the design of robots including collaborative robots. In order to make the interaction between robots and humans more intuitive, robots need to be smart enough to react to changes produced by their human collaborator properly, which can be achieved through the exchange of sensory feedback: including visual observation of the motion dynamics, and haptic observation of the interaction force between the body and external environment. The best way to achieve a high level of action recognition in design of robots is to first discern the underlying neural mechanism behind the human sensorimotor system.

The central nervous system (CNS) receives a continuous stream of sensory information from multiple modalities and sends appropriate motor commands to our muscles. In other words, the sensory and motor systems intimately interplay as a closed-loop feedback system. However, the sensory feedbacks gathered from various modalities are often noisy and delayed, which may challenge the CNS to control our movements. Due to the delayed nature of our sensory and motor systems, we live in the past and our control system is limited to outdated information about our body and environment. Sometimes the movement duration is shorter than the sensory delay, and it might cause the control system to correct for those errors that no longer exist and lead the system to instability⁷⁷.

On the other hand, humans have a complex body structure with typically more degrees of freedom (DOF) (i.e., motor effectors) than is required for a successful task performance¹³. Therefore, theoretically, each motor task can be performed in an endless number of ways³⁷. One of the biggest issues in motor control is that how CNS manages to select a solution from many apparently similar alternatives for performing a motor task¹³. There have been many attempts to

answer the DOF problem. Among all these attempts, a well-defined theory known as optimal feedback control theory⁵⁶ states that CNS sets up feedback controllers that continuously convert sensory input to motor output. This theory is based on the principle of minimum intervention, indicating that feedback controllers are set up in a way that corrects for only those deviations that intervene the task^{56,77}. So that, it can handle possible perturbations sensed by sensory systems. In other words, CNS does not look for a single optimal solution; it preferably utilizes a family of solutions known as synergies with error compensation characteristics to ensure the stability and flexibility of performance²³. So, instead of redundancy, we have abundance in the human motor system¹².

However, how CNS integrates noisy sensory information and uses them to synergistically control its redundant motor elements for successful task performance has not become clear yet. Empirical studies have provided convincing evidence that we, human, optimally combine information from multiple sensory modalities in a way to enhance the perception, which may be best described by Bayesian integration^{78,79}. Ernst and Banks have shown that humans integrate visual and haptic information in a statistically optimal manner based on the maximum-likelihood integrator. More specifically, visual and haptic information is weighted by the inverse of their variances, which reflect the reliability of each sensory modality. So, the more reliable modality contributes more to the information fed back to CNS to enhance the perception. It has been reported that there exist multimodal neurons in premotor, parietal, and subcortical areas of the brain. The neurons responded stronger³³ and faster⁸⁰ by the presence of multisensory stimuli than that of unisensory stimuli. It also has been found that reaction time in response to visual and tactile stimuli are faster than those to unimodal stimuli³².

There have been several studies conducted to develop neural mechanism models of sensorimotor interactions and synergistic control⁸¹ scheme by incorporating modern control technologies such as feed-forward control⁸², pure feedback control, optimal feedback control⁵⁶, adaptive control⁸³, neural network⁸⁴, etc. However, none of them have shown the relation between sensory integration and motor synergy associated with motor redundancy (or abundance). Therefore, in this paper, the effect of sensory information integration onto the synergetic control technique will be discussed by simulating the multi-finger force production task. We incorporated the proposed characteristics that have been shown to exist in empirical studies of finger force production, such as sharing, lateral inhibition, and enslaving into our model. Finally, we have used Bayesian integration in our model to explain how CNS utilizes sensory information that receives from multiple modalities to control movement.

The primary goal of the proposed model is to predict the most probable behavior from a set of observed behaviors under two conditions: in the presence vs. absence of tactile feedback. We chose the action of finger force production since the multi-digit finger motion is one of the representative synergetic movements in the human body. Our goal of modeling this sensorimotor system is to reveal potential systematic mechanisms employed by the CNS to control our movement, and to gain insight for clinical applications or control design of co-working robots.

5.3 Methods

5.3.1 Multi-Digit Finger Force Production: Experimental Data

5.3.1.1 Participants

The experimental data that has been used here is collected from 18 healthy participants (sex: males, age: 23.95 ± 1.00 years, body mass: 68.00 ± 5.21 kg, height: 174.67 ± 5.59 cm) with no

history of neurological disorders. All the participants were right-handed according to the Edinburgh handedness test criteria. The hand length measured from the middle fingertip to the lunate of the wrist was 17.2 ± 1.0 cm, and the hand width measured across the metacarpophalangeal (MCP) joints of the index and little fingers was 9.5 ± 0.6 cm. All the participants gave informed consent based on the procedures approved by Korea University Institutional Review Board.

5.3.1.2 Experimental setup

Participants were asked to rest the distal phalanges of each of the four fingers of their right hand on force sensors (Models 208 M182 and 484B, Piezotronics, Inc., Depew, NY), such that all joints were slightly flexed and the hand formed a dome shape. To minimize any tactile feedback from the palm, the palmar surface and the fingers were not restrained physically. Full details of the experimental setup can be found in our previous study⁸⁵.

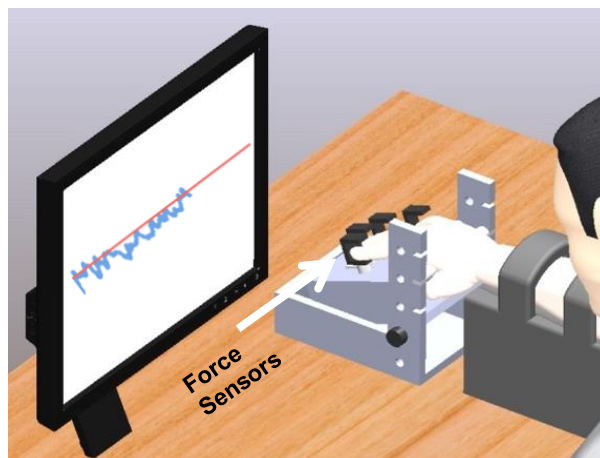


Figure 5.1. Experimental Setting

Each participant performed the task under two conditions: in the presence versus absence of tactile feedback. Each condition consisted of 12 trials, in each of which the subject was asked

to produce a constant force of 20 N (total end-point fingertip forces, summed over all four fingers) over 12 seconds. The subject was shown the force produced by his/her fingers along with the target force in the form of a horizontal bar on a computer screen (Figure 5.1). The two conditions were administered on two different days in a balanced order. On the day of experiment in the presence of tactile feedback, each subject performed the trials with his/her normal tactile sensation. On the day of the experiment in the absence of tactile feedback, the tactile feedback was removed by first applying a topical anesthetic (Dermacain Cream 5%, Hana Pharm Co., Ltd., Seoul, Korea) to the middle phalanges of each finger, and then injecting a local anesthetic (Lidocaine HCl 1%, DaiHan Pharm. Co., Ltd., Seoul, Korea) at four sites around the middle phalanges of each finger (3.5 cc. for index, middle and ring fingers; 2.5 cc. for little finger) 5 minutes later. The injection was followed by a stroking massage in the direction of distal phalanges.

5.3.2 Multi-Digit Finger Force Production: Mathematical Model

The proposed feedback model consists of a controller to perform the control role of CNS, effectors to resemble finger dynamics and sensors for including the tactile and visual feedback mechanisms (Figure 5.2). We used Proportional, integral, derivative (PID) controller to resemble the control role of CNS, where the proportional component of it contributes to controlling the response time of the system as it changes the force from zero to target force. The integral part could be interpreted as the memory where it restores the past data and uses them in the present to reduce the steady-state response. Finally, the derivative part contributes to enhancing the stability of the system. The CNS compares the desired versus sensed multi-digit forces at a higher level and determines the forces required to be produced by each finger. The fingers then produce these requisite forces, and the resultant multi-digit force is obtained by adding up the individual finger forces. The tactile sensors in the fingers measure individual finger forces, while the visual sensors

(eyes) measures the resultant force. These sensor measurements are finally integrated and fed back to the CNS, which then determines the compensatory finger forces based on motor synergy theory and central back coupling model⁸⁶ to eliminate the error between desired versus actual multi-digit finger forces. This feedback block diagram is consistent with biological knowledge that (1) the CNS integrates the sensory information to plan motion and produce control commands to each motor to accomplish a required task at a higher level, (2) the tactile information is transmitted to the CNS via the peripheral (median, ulnar and radial) nerves at each finger, and integrated with the visual information that is transmitted to the CNS directly.

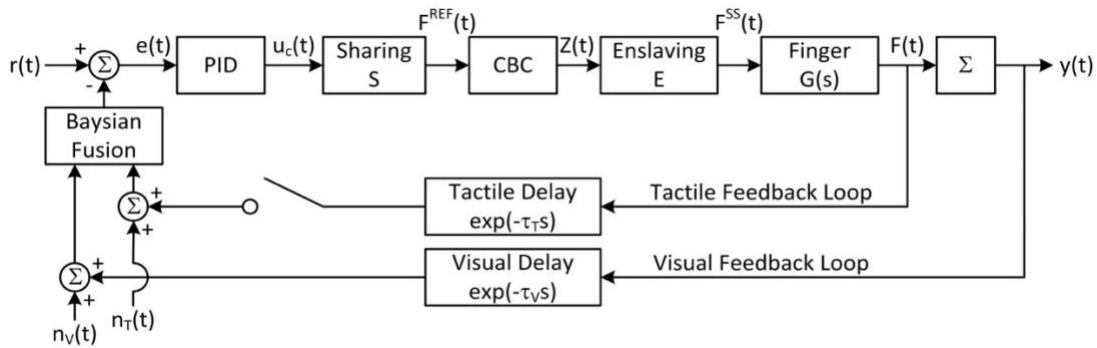


Figure 5.2. The proposed feedback control model block diagram for finger force production task

To include the synergetic aspect of the sensorimotor system into the model, the following plants were added to it: sharing, lateral inhibition, and enslaving⁸⁷. The sharing function dictates how the resultant compensatory finger force (u_c) should be allocated to each finger (i.e., lower level of control). Force sharing characteristic is one of the examples of redundancy problem where different combinations of force can produce the same total force. Denoting the output of the sharing function as the reference force to be produced at each finger f_k^{REF} ($k = 1, 2, 3, 4$ where 1, 2, 3 and 4 indicate index, middle, ring, and little fingers), the sharing function was modeled as a vector of constants:

$$\mathbf{F}^{\text{REF}} = \begin{bmatrix} f_1^{\text{REF}} \\ f_2^{\text{REF}} \\ f_3^{\text{REF}} \\ f_4^{\text{REF}} \end{bmatrix} = \mathbf{S} \mathbf{u}_c = \begin{bmatrix} s_1 \\ s_2 \\ s_3 \\ s_4 \end{bmatrix} \mathbf{u}_c \quad (1)$$

where $s_1 + s_2 + s_3 + s_4 = 1$.

The CBC function represents synergistic behaviors that are common in neuro-physiological systems⁸⁸, such as auto- and cross-inhibition of finger forces and interaction delays occurring in multi-digit coordination tasks. The model developed by Latash and colleagues⁸⁶ was used in this study, which is a feedback system consisting of a unity forward-loop gain and a negative feedback-loop gain (Γ) with transport delay (Figure 5.3):

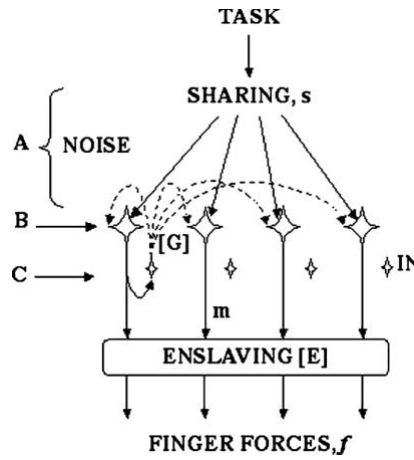


Figure 5.3. Schematic of CBC model taken from⁸⁶

$$\mathbf{Z} = \begin{bmatrix} z_1 \\ z_2 \\ z_3 \\ z_4 \end{bmatrix} = (\mathbf{I}_{4 \times 4} - e^{-\tau_{\text{CBC}} s} \Gamma)^{-1} \mathbf{F}^{\text{REF}} = \left(\mathbf{I}_{4 \times 4} - e^{-\tau_{\text{CBC}} s} \begin{bmatrix} g_{11} & \cdots & g_{14} \\ \vdots & \ddots & \vdots \\ g_{41} & \cdots & g_{44} \end{bmatrix} \right)^{-1} \mathbf{F}^{\text{REF}} \quad (2)$$

where \mathbf{Z} is the output of CBC, $\mathbf{I}_{4 \times 4}$ is an identity matrix, s is the Laplace variable, τ_{CBC} is the transport delay associated with the neural pathways, and g_{ij} ($1 \leq i, j \leq 4$) denotes the inhibitory interaction between fingers i and j .

The enslaving function is included to account for the fact that activation of a finger elicits co-activation of other fingers due to the physical interconnection between them⁸⁷. This function was modeled as a constant matrix gain (E):

$$F^{SS} = \begin{bmatrix} f_1^{SS} \\ f_2^{SS} \\ f_3^{SS} \\ f_4^{SS} \end{bmatrix} = EZ = \begin{bmatrix} e_{11} & \cdots & e_{14} \\ \vdots & \ddots & \vdots \\ e_{41} & \cdots & e_{44} \end{bmatrix} Z \quad (3)$$

where the output of the enslaving function F^{SS} denotes the forces at individual fingers that would be produced if the dynamics of the fingers were negligible.

The dynamic response of the fingers was modeled as a second-order linear system: We considered digit motion along only one direction and assumed a linear damped second-order model (one degree-of-freedom)⁸⁹:

$$F = \begin{bmatrix} f_1 \\ f_2 \\ f_3 \\ f_4 \end{bmatrix} = G(s)F^{SS} = \begin{bmatrix} G_1(s) & 0 & 0 & 0 \\ 0 & G_2(s) & 0 & 0 \\ 0 & 0 & G_3(s) & 0 \\ 0 & 0 & 0 & G_4(s) \end{bmatrix} F^{SS} \quad (4)$$

where F is the vector of individual finger forces, $G_k(s) = K\omega_{n,k}^2 / (s^2 + 2\zeta_k\omega_{n,k}s + \omega_{n,k}^2)$, and ζ_k and $\omega_{n,k}$ are damping ratio and natural frequency associated with $G_k(s)$ ($k = 1,2,3,4$). In sum, the control command u_c from the CNS is related to the individual finger forces F as follows:

$$F(s) = G(s)E(I_{4 \times 4} - e^{-\tau_{CBC} s} \Gamma)^{-1} S u_c(s) \quad (5)$$

where $F(s)$ and $u_c(s)$ are explicitly expressed as functions of s for clarity.

The sensory feedback signal transmitted to the CNS ($y(t)$) was modeled as the Bayesian integration of visual and tactile feedback⁷⁹:

$$y(t) = \mathcal{B}(y_V(t), y_T(t)) = \frac{1/\sigma_V^2}{1/\sigma_V^2 + 1/\sigma_T^2} y_V(t) + \frac{1/\sigma_T^2}{1/\sigma_V^2 + 1/\sigma_T^2} y_T(t) \quad (6)$$

where $\mathcal{B}(\cdot)$ is the Bayesian sensory fusion function, while $y_V(t)$ and $y_T(t)$ are the visual and tactile sensory signals, respectively. As shown in Figure 5.2, the visual sensory system measures the resultant multi-digit finger force as displayed on the screen (Figure 5.1) while the tactile sensory system measures the forces produced at the individual finger level. Noting that both sensory feedback mechanisms involve measurement noise and transport delays along their neural pathways⁹⁰, and also that the CNS applies the Bayesian sensory fusion to the resultant multi-digit finger forces to determine the compensatory force u_c , $y_V(t)$ and $y_T(t)$ can be written as follows:

$$y_V(t) = \left[\sum_{k=1}^4 f_k(t - \tau_V) \right] + n_V(t), \quad y_T(t) = \sum_{k=1}^4 [f_k(t - \tau_T) + n_{T,k}(t)] \quad (7)$$

where τ_V and τ_T are the transport delays associated with visual and tactile sensory pathways, and $n_V \sim \mathcal{N}(m_V, \sigma_V^2)$ and $n_{T,k} \sim \mathcal{N}(m_{T,k}, \sigma_{T,k}^2)$ are the noises associated with visual and tactile sensory systems, where m and σ denote the mean and standard deviation of the noise distribution. The input to the CNS (e) is given by the error between the reference (r ; as given by the horizontal bar displayed on the screen) versus Bayesian-integrated multi-digit finger force signals (Figure 5.2):

$$e(t) = r(t) - y(t) = r(t) - \mathcal{B}(y_V(t), y_T(t)) \quad (8)$$

In the absence of a widely accepted feedback control model of CNS, the control action in the CNS to determine u_c was modeled as a generic proportional-integral-derivative (PID) controller:

$$u_c(t) = K_P e(t) + K_I \int e(t) dt + K_D \frac{de(t)}{dt} \quad (9)$$

where K_P , K_I and K_D are PID controller gains.

5.3.3 Multi-Digit Finger Force Production: Simulation

To reproduce the multi-digit finger force production task using the mathematical model described in section 5.3.2 Multi-Digit Finger Force Production: Mathematical Model, the parameters in the mathematical model were assigned as follows. The parameters in the sharing function S in (1) were chosen based on the experimental data. From each trial, the data from 5 to 11s was extracted (to avoid the initial force stabilization in the beginning of each trial and premature cessation of force production at the end^{5,53}). Then, the sharing parameters s_k , $k = 1,2,3,4$ corresponding to each trial were determined as the normalized time-averaged finger force:

$$\bar{s}_k = \frac{\overline{f_k(t)}}{\overline{f_1(t)} + \overline{f_2(t)} + \overline{f_3(t)} + \overline{f_4(t)}} \quad (10)$$

where $\overline{f_k(t)}$ is the time-averaged force at the finger k . In simulating each trial, a zero-mean Gaussian noise was added to the sharing function to account for the fact that s_k contains small-amplitude random fluctuations: $s_k = \bar{s}_k + n_{s,k}$, where the noise level was set proportional to the sharing with standard deviation of sum of forces in each trial. In addition, frequency analysis of the experimental data suggested that the behavior of the signals is different at different frequencies. Frequency domain measures (spectral analysis) have identified the existence of in-phase and anti-phase patterns of coordination between each pair of fingers at different frequencies. In particular, the complex coherence⁷⁶ analysis revealed that error compensation, one of the features of motor synergies, is occurring at low frequencies. Complex coherence (i.e., a vector of complex values that measures the linear relationship between two signals at different frequencies) between each pair of finger forces including index-middle, index-ring, etc. was calculated as:

$$\text{Complex coherence} = \frac{CSD_{x,y}}{\sqrt{PSD_x PSD_y}} \quad (11)$$

In this equation, $CSD_{x,y}$ represents the cross spectral density between signal x and y and PSD_x and PSD_y are power spectral densities of signal x and y, respectively. From this equation, magnitude squared coherence (i.e., the absolute value squared of complex coherence) and phase of complex coherence were extracted and plotted for the duration of the trial, where the total force was almost stationary (5-11s). As Figure 5.4 demonstrates, at low frequencies (below 1 Hz), the signals are anti-phase. This denotes that at low frequencies, every two pairs of signals are negatively correlated. Although coherence is fairly low (about 0.1) at these frequencies, the power of signals and CSD between each two signals were high. As we move to higher frequencies (1.6Hz-2.5Hz), the coherence becomes higher (around 0.4), power become very close to zero, and phase shift between two signals at these frequencies is almost zero, denoting that at higher frequencies, the two signals are positively correlated with each other. A negative correlation between two signals shows the error compensation between fingers that ensures the stability of task performance at higher level. Given that the power of signals is high at low frequencies, the overall sum of covariances within a trial become negative, which ensures the stability at task level. In order to implement these results in the model, we added colored noise to the sharing function and made it time-varying within a trial. A few studies⁹¹⁻⁹³ have shown that CNS uses the inherent noise for the coordination of its effectors and this noise has a property of pink noise whose power spectral density follows power law (1/f). So, we added a pink noise to our sharing function.

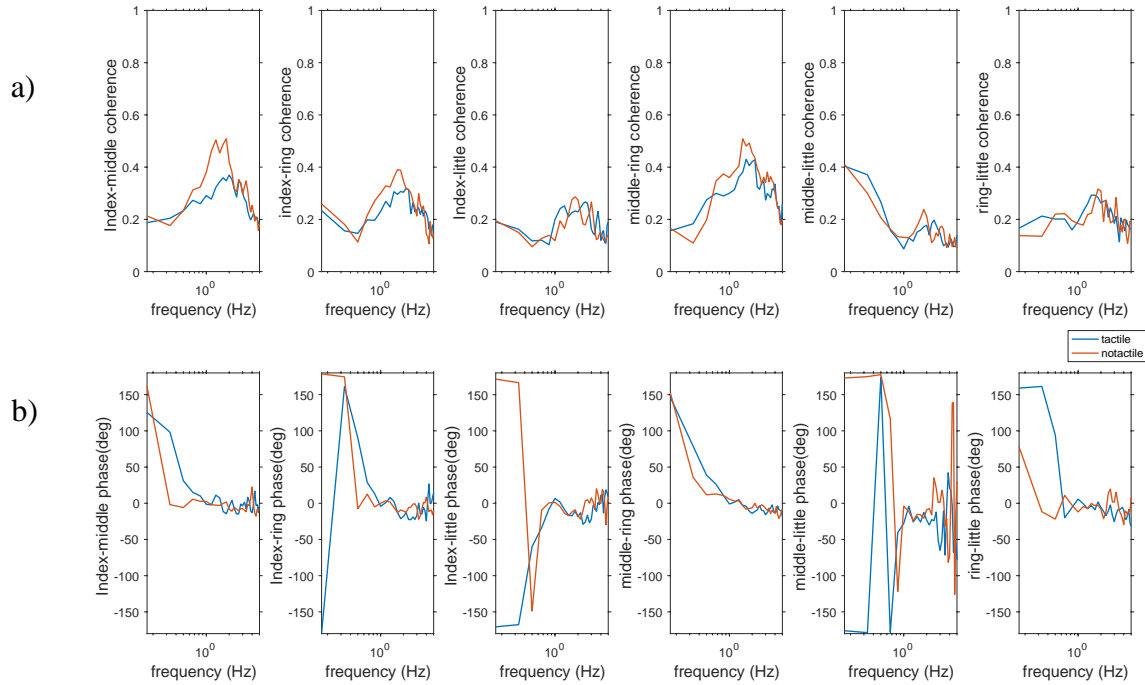


Figure 5.4. Complex coherence. a) magnitude squared coherence. b) phase of complex coherence

The initial parameter values for the CBC model were chosen based on the previous studies⁸⁶, and they were further tuned so that the mathematical model could better reproduce the experimental data. The final values used were $g_{ij} = 0.13$ ($1 \leq i, j \leq 4$) and $\tau_{CBC} = 10$ ms, which are close to the values reported in the literature⁸⁶. The enslaving function was adopted from a previous study⁸⁷. The sensory noises were assumed to be zero-mean, and the variance parameters were found based on the experimental data. The tactile sensory feedback delay (τ_T) was set to 40 ms based on its typical values reported in the literature³². In accordance with the results reported in previous behavioral science studies (which reported that minimum sensory transduction delay required for a visual or proprioceptive signal to influence an ongoing movement is about 80-100 ms⁹⁰), the visual sensory feedback delay (τ_V) was set to 100 ms when the tactile feedback is absent. However, both of them were set to τ_T (40 ms) when the tactile feedback is present, noting that the CNS responds to sensory signals faster^{94,95}.

With the parameters chosen above, the remaining parameters associated with the finger dynamics (4) (ζ_k and $\omega_{n,k}$, $k = 1,2,3,4$) and the initial values for PID controller (9) were chosen via system identification⁹⁶, so that the experimental force responses associated with individual fingers ($f_k(t)$, $k = 1,2,3,4$) could be reproduced by the model's simulated finger force responses. The experimental data suggested that force responses produced by all the fingers exhibited similar oscillation and speed characteristics. Based on the defined parameters, individual finger forces were simulated for each subject and each trial. To identify PID parameters for different subjects, conditions, and trials, an optimization problem with an objective of minimization of root mean square error between sum of simulated finger forces (f_{simi}) and target force (20N) was solved:

$$J = rms\left(\sum_{i=1}^4 f_{simi} - 20\right) \quad (12)$$

The main reason for solving this optimization problem was to examine if we gather all the information from previous studies in a model, it would successfully complete the task goal of the experiment and it would reproduce the experimental data and more specifically the synergistic interaction between fingers.

5.3.5 The role of tactile sensory feedback in multi-finger synergy

To elucidate how the within-trial variance and synergy associated with the individual finger forces in (13a) decreases when the tactile sensory feedback is removed, the proposed mathematical model was analyzed in more detail. First, the feedback block diagram in Figure 5.2 is reduced to Figure 5.5a when the tactile sensory feedback is removed, which can be obtained by eliminating the tactile feedback loop from Figure 5.2. Here, the Bayesian sensory fusion reduces to unity. In contrast, when the tactile sensory feedback is present, Figure 5.2 can be modified to Figure 5.5b, by rewriting the Bayesian sensory fusion function as follows:

$$\begin{aligned}
y(t) &= \frac{1/\sigma_V^2}{1/\sigma_V^2 + 1/\sigma_T^2} y_V(t) + \frac{1/\sigma_T^2}{1/\sigma_V^2 + 1/\sigma_T^2} y_T(t) \\
&= y_V(t) + \frac{1/\sigma_T^2}{1/\sigma_V^2 + 1/\sigma_T^2} (y_T(t) - y_V(t)) \\
&= y_V(t) + \frac{1/\sigma_T^2}{1/\sigma_V^2 + 1/\sigma_T^2} \left(\sum_{k=1}^4 n_{T,k}(t) - n_V(t) \right)
\end{aligned} \tag{13}$$

where the last equality holds since $\tau_T = \tau_V$ when the tactile sensory feedback is present.

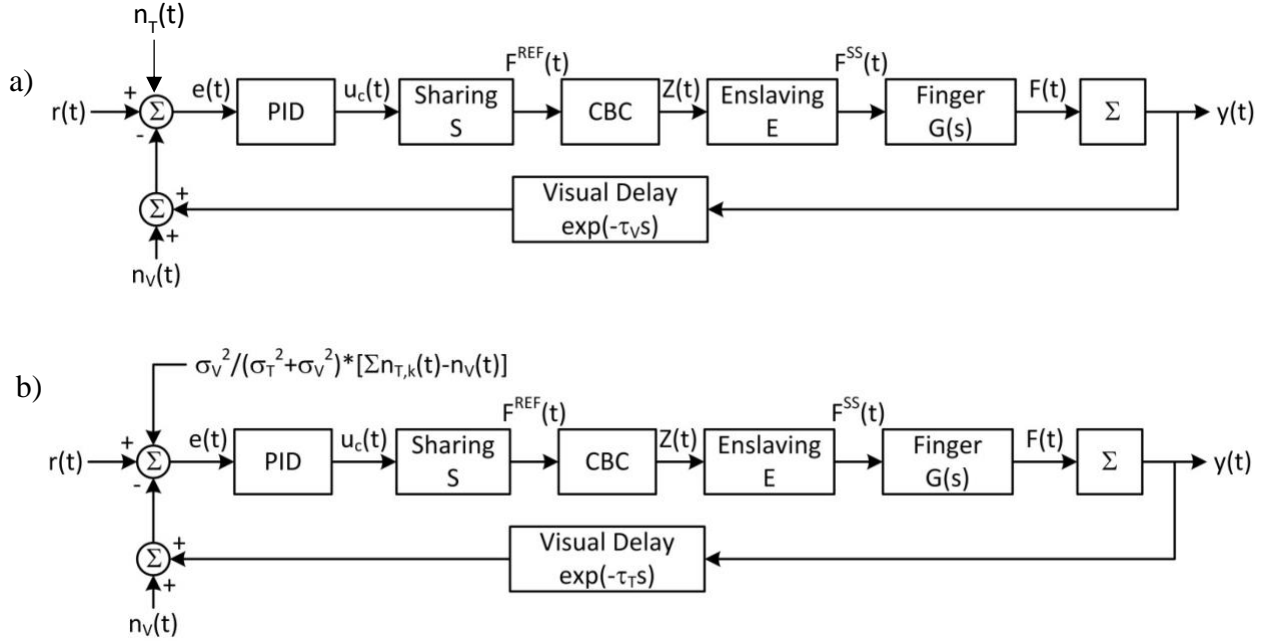


Figure 5.5. Equivalent feedback control block diagram of the multi-digit finger force production task in the (a) absence (b) presence of tactile sensory feedback.

However, after removing the tactile loop, we kept the noises associated with tactile sensory feedback as the uncertainty in perception of the force increases after removal of tactile feedback.

5.3.5 Data Analysis

To investigate the role of tactile sensory feedback on the synergy between multiple fingers, the data collected from experiments and simulations were analyzed according to hierarchical variability decomposition approach (HVD)²⁵. Based on this approach, the task performance, was quantified in terms of the overall mean-squared error (OMSE) and decomposed to within-trial

(called “online” $\overline{\text{Var}(\tilde{y})}$) and trial-to-trial (called “offline” $\text{Var}(\varepsilon)$) variances of the resultant finger force, and systematic error $((r - m)^2)$ as:

$$\text{OMSE} = \frac{1}{N} \sum_{i=1}^N \frac{1}{\tau} \int_{t=0}^{\tau} [r(t) - y_i(t)]^2 dt = \overline{\text{Var}(\tilde{y})} + \text{Var}(\varepsilon) + (r - m)^2 \quad (13)$$

The variances for the resultant finger force were further decomposed into the individual finger level as follows:

$$\overline{\text{Var}(\tilde{y})} = \overline{\text{Var}\left(\sum_{k=1}^4 \tilde{f}_k\right)} = \sum_{k=1}^4 \overline{\text{Var}(\tilde{f}_k)} + \sum_{j \neq k}^4 \overline{\text{Cov}(\tilde{f}_j, \tilde{f}_k)} \quad (14a)$$

and

$$\text{Var}(\varepsilon) = \text{Var}\left(\sum_{k=1}^4 \varepsilon_k\right) = \sum_{k=1}^4 \text{Var}(\varepsilon_k) + \sum_{j \neq k}^4 \text{Cov}(\varepsilon_j, \varepsilon_k) \quad (14b)$$

where \tilde{f}_k and ε_k are demeaned force and force averaged over time, respectively, corresponding to the finger k. In (14), the covariance terms represent the within-trial (14a) and trial-to-trial (14b) interactions of multiple fingers during force production, thus they were used as measure of multi-finger synergy associated with the force production task.

For each subject, OMSE was analyzed both in the presence and absence of tactile sensory feedback. In each trial, the data segment from 5 to 11 seconds was extracted to analyze OMSE. The influence of tactile sensory feedback on multi-finger synergy was examined by analyzing the OMSE and its components. The influence of tactile sensory feedback on multi-finger synergy was examined by analyzing the OMSE and its components (including the variance and covariance terms in (13)) in the presence and absence of tactile sensory feedback. Two-way repeated measures ANOVA was used to assess the statistical significance in the difference between model and experiment in the two conditions. The level of statistical significance was set to $p=0.05$.

5.4 Results

5.4.1 Finger Force Trajectories

Figure 5.6 shows a representative resultant and individual finger force responses simulated by the model (Figure 5.2) in the (a) presence and (b) absence of tactile sensory feedback. Both simulation and experiment show that if one of the finger forces varies independently with predefined sharing ratio, other finger forces are also cooperatively varied to track the reference summation force.

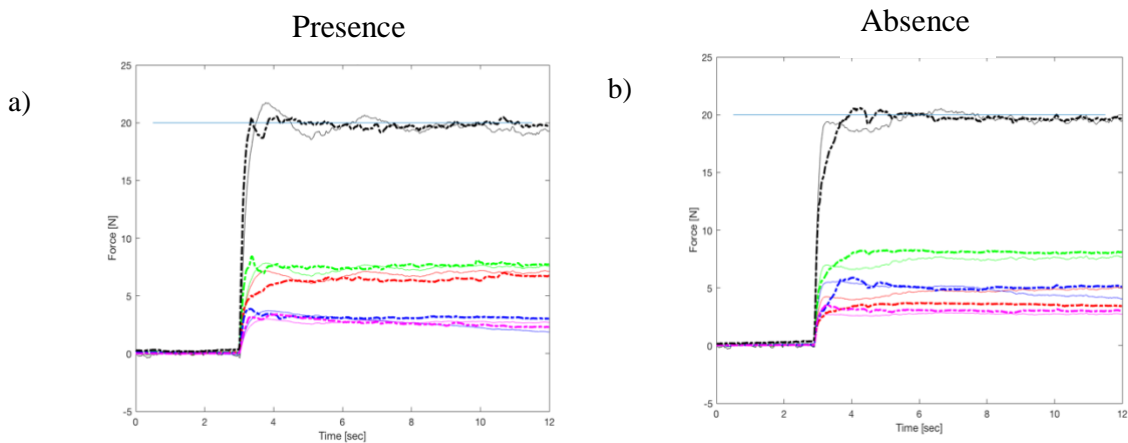


Figure 5.6. Simulated and experimental resultant (i.e., black line) and individual finger forces for a) presence of tactile feedback, b) absence of tactile feedback. In both conditions, the solid lines represent the experiment and the dash lines represent the simulation

5.4.2 Synergistic Interaction between fingers through HVD analysis

Figure 5.7 compares the result of the simulation with experimental results using HVD analysis. In all levels of the hierarchy, simulation results could reproduce the experimental trend. The highest level of hierarchy, including mean square error, online and offline variances and systematic error remained unchanged after removal of the tactile loop. In contrast, between-finger synergy decreased after removal of tactile feedback in both experiments and simulation.

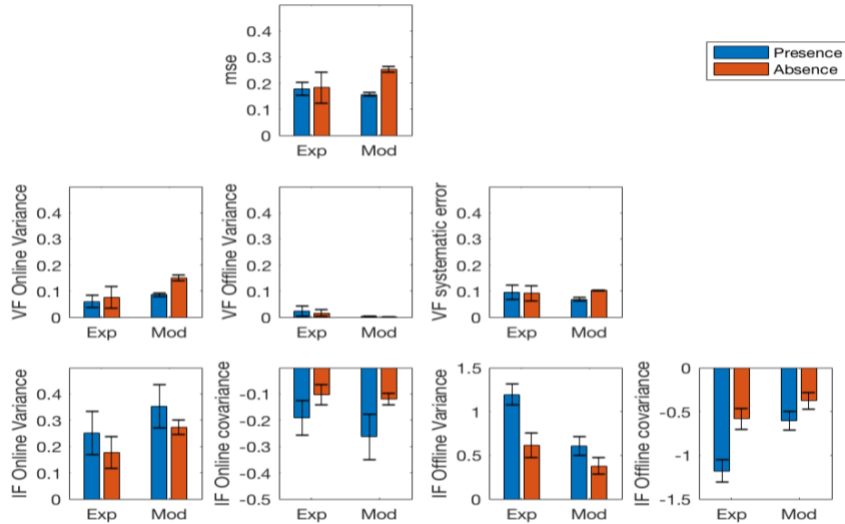


Figure 5.7. The HVD analysis for the experiment and simulation. The blue bars show the presence and the red bars show the absence of tactile feedback

5.5 Discussion

We investigated the role of sensory integration on the synergetic behavior of redundant motor control by studying multi-digit finger force production task. The task was established on human subject experiment, and the experiment-based feedback control scheme simulation was presented. The experimental and simulation results showed that the synergetic control performance is enhanced when the tactile feedback is provided to the CNS. The feedback control model presented in this paper, simulates finger force matching task under two conditions. Using this experiment-based model, we explained how inherently noisy and delayed sensory and motor systems can interplay in a closed-loop structure to perform a task. In a former work done by our research team²⁵ using analytical techniques, we showed that tactile sensors play a substantial role in the synergistic interactions between fingers within each trial but not between trial. Furthermore, the combined motor output of individual fingers remains the same in both conditions, which

supports the theory of the hierarchical control where individual fingers at lower level are coupled to produce a stable motor output at the higher level.

In this paper, we mainly looked for the underlying neural mechanism behind this phenomenon using a gray box model which explains how the noisy and delayed neural command utilizes the integrated multisensory information. Although it is impossible to reproduce the exact force variation profile in the time domain of experiment onto simulation, the derived model was able to reproduce experimental data as shown in Figure 5.6. As we can see, the model could reproduce the experimental results in which the removal of tactile feedback was associated with the decreased individual finger force variability and decreased negative covariance (i.e., synergy). The absence of tactile feedback introduces instability to the system, but unchanged variability in the sum of the forces (task performance) shows that CNS compensate for this instability by changing the coupling between finger forces. Previous studies⁸⁶ described a central back coupling scheme where short-latency negative feedback loops can mimic the action of a synergy without any need for sensory feedback. In this scheme, there are inhibitory connections between the elements so that an increase in activity of one element leads to a decrease in the others. This effect leads to compensation between the elements without the need for sensory feedback. Similarly, Goodman and Latash⁸² proposed that compensation can be observed in a purely feedforward control scheme as long as the controller has information about the relationship between the change in the output to the changes in the individual elements (i.e., the Jacobian of the system). However, our model showed that central back coupling alone is not sufficient to explain the reduction in synergy after removal of tactile feedback. This model further suggests that the derived feedback control model of sharing, CBC, enslaving and Bayesian multisensory integration, all together, can explain important components of the CNS control strategy for the control of redundant tasks even

after removal of one sensory modality. This result confirms with Todorov and Jordan⁵⁶'s principle of minimal intervention and the important role of sensory feedback on the formation of these variability patterns. This theory states that CNS uses feedback to correct deviations that interfere with the task goal but allows variability in redundant dimensions.

Limitation: One of the limitations of this model is the use of the PID controller with gain optimization for experimental result explanation. This may not be the best representative of control aspect of CNS. However, we tried to incorporate other components of sensorimotor system to reflect some of the critical control aspects of CNS. In addition, since we have a steady-state process, a PID controller was a reasonable choice. However, some discrepancies between the time course response of the simulation and experiments could be due to the use of this type of controller. Another limitation of our model is related to our estimation of the mechanical parameters within the second-order linear model. This was an obvious simplification of the real object and inadequacy of such linear models has been emphasized⁸⁷. However, even with these simplifications, we could reproduce the synergistic interaction between fingers and explain some of the crucial features of CNS in completing this redundant action.

5.6 Future Directions

Modeling Human-Human Sensorimotor Interaction

We aim to extend our model of single person performing multi-finger force tracking task²⁵ to two-person task using the experimental data that we collect in experiment I. From the spectral analysis explained in Chapter 4 and experiment on Human-Human interaction, we found that we could predict the closed-loop behavior from open-loop, and the behavior of people in response to another person or a disturbance did not defer. Therefore, as the first step toward modeling Human-Human interaction, we can consider the other person as an environmental disturbance and see if

our model of single-person reacts to it correctly or not. This model could be beneficial for human-robot interaction field, where robots can interact with users more intuitively.

Appendices

Relation between HVD and Uncontrolled Manifold

The following is the proof of how hierarchical variability decomposition method is related to uncontrolled manifold theory. Specially, how negation of covariance is the same as index of synergy.

$$F_{total} = F_{P_1} + F_{P_2}$$

$$F_{P_j} = f_{index_j} + f_{middle_j} = \overset{\circ}{\underset{i=1}{\overset{2}{\mathbf{a}}}} f_i$$

$$\overline{\overline{F_{total}}} = \frac{1}{10} \overset{\circ}{\underset{T=1}{\overset{10}{\mathbf{a}}}} \overline{\overline{F_{total}}}(T)$$

$$MSE = \overline{\overline{Var(F_{total})}} + \overline{\overline{Var(F_{total})}} + (20 - \overline{\overline{F_{total}}})^2$$

$$MSE = \overline{\overline{Var(\overset{\circ}{\underset{i=1}{\overset{2}{\mathbf{a}}}} f_i)}} + \overline{\overline{Var(\overset{\circ}{\underset{i=1}{\overset{2}{\mathbf{a}}}} \overline{f_i})}} + (20 - \overline{\overline{F_{total}}})^2$$

$$MSE = \overset{\circ}{\underset{i=1}{\overset{2}{\mathbf{a}}}} \overline{\overline{Var(f_i)}} + \overset{\circ}{\underset{i^1k}{\overset{2}{\mathbf{a}}}} \overline{\overline{Cov(f_i, f_k)}} + \overset{\circ}{\underset{i=1}{\overset{2}{\mathbf{a}}}} \overline{\overline{Var(\overline{f_i})}} + \overset{\circ}{\underset{i^1k}{\overset{2}{\mathbf{a}}}} \overline{\overline{Cov(\overline{f_i}, \overline{f_k})}} + (20 - \overline{\overline{F_{total}}})^2$$

$$\setminus \overline{\overline{Var(\overset{\circ}{\underset{i=1}{\overset{n}{\mathbf{a}}}} X_i)}} = \overset{\circ}{\underset{i,k=1}{\overset{n}{\mathbf{a}}}} \overline{\overline{Cov(X_i, X_k)}} = \overset{\circ}{\underset{i=1}{\overset{n}{\mathbf{a}}}} \overline{\overline{Var(X_i)}} + \overset{\circ}{\underset{i^1k}{\overset{n}{\mathbf{a}}}} \overline{\overline{Cov(X_i, X_k)}}$$

Where f_i is an i th finger force.

Let's say f_{\parallel} and f_{\wedge} are force data in UCM space and in orthogonal to the UCM space, respectively:

$$\sum_{i=1}^n Var(f_i) = Var(f_{\parallel}) + Var(f_{\perp})$$

$$Var(f_{\perp}) = \frac{1}{n} Var(\sum_{i=1}^n f_i),$$

$$Var(f_{\parallel}) = \sum_{i=1}^n Var(f_i) - \frac{1}{n} Var(\sum_{i=1}^n f_i).$$

$$\overline{Var(f_{\parallel})} = \sum_{i=1}^n \overline{Var(f_i)} - \frac{1}{n} \overline{Var(\sum_{i=1}^n f_i)}$$

$$Var(\overline{f_{\parallel}}) = Var(\sum_{i=1}^n \overline{f_i}) - \frac{1}{n} Var(\sum_{i=1}^n \overline{f_i})$$

n refers to degrees of freedom in the system and it is equal to 2 in our case.

And Synergy between effectors in neuromechanically redundant system, according to UCM method, is defined as the differences in effector variance in the task-irrelevant space (online:

$\overline{Var(f_{\parallel})}$, offline: $Var(\overline{f_{\parallel}})$) that characterizes the CNS's utilization of redundant degrees of

freedom, and the task-irrelevant space (online: $\overline{Var(f_{\wedge})}$, offline: $Var(\overline{f_{\wedge}})$) that specifies the

motor task error. Based on the formulation shown above and this definition, it is proved that the

calculation of motor synergies employed in previous studies is the simple negation of covariance.

$$Syn(f) = \overline{Var(f_{\parallel})} - (n-1)\overline{Var(f_{\perp})} = -\sum_{i \neq k} \overline{Cov(f_i, f_k)}$$

$$Syn(\overline{f}) = Var(\overline{f_{\parallel}}) - (n-1)Var(\overline{f_{\perp}}) = -\sum_{i \neq k} Cov(\overline{f_{\parallel}}, \overline{f_{\perp}})$$

$Syn(f)$ and $Syn(\overline{f})$ are the indices of intra-trial and inter-trial synergy between finger forces,

which we denote online and offline synergy, respectively.

Personality Questionnaire

In human-human interaction experiments, We asked participants to fill out a 50-item questionnaire which measures personality factors according to the 50-item International Personality Item Pool (IPIP) representation of the Goldberg markers for the Big-Five factor structure (i.e., extraversion, neuroticism, agreeableness, conscientiousness, and openness to experience⁹⁷. We were interested in understanding if the control strategies that people tend to choose correlated with their personality. In other words, to examine if we can predict people's behavior in our co-working task based on the scores of their personality traits. We ran a regression analysis to fit a model with the score of participants in any of these five big factors as predictors and all the HVD variables including the online and offline covariance (which was used to measure coordination strategy) as the outcome. However, we did not find any significant correlation coefficient, indicating that we could not predict people's behavior based on these personality traits.

Predicting closed-loop behavior from open-loop conditions

The following equations show how we calculated the PSD of force in closed-loop condition from the open loop conditions:

$$H_1 = \frac{F_1}{F_2}, H_2 = \frac{F_2}{F_1}$$

$$F_1 = H_1 F_2 + N_1, F_2 = H_2 F_1 + N_2$$

$$F_1 = H_1(H_2 F_1 + N_2) + N_1 \Rightarrow (1 - H_1 H_2) F_1 = H_1 N_2 + N_1 \Rightarrow F_1 = \frac{H_1 N_2 + N_1}{(1 - H_1 H_2)}$$

$$PSD \text{ of } F_1 = \frac{H_1 P_{N_2 N_2} + P_{N_1 N_1}}{(1 - H_1 H_2)}$$

F_1 and F_2 are the forces of P_1 and P_2 , respectively. H_1 and H_2 are the FRFs (taken from open-loop conditions), and N_1 and N_2 are the additional noises in the system of P_1 and P_2 , respectively. $P_{N_1N_1}$ and $P_{N_2N_2}$ are the conditioned PSDs for P_1 and P_2 , respectively.

Bibliography

1. SEBANZ, N., Bekkering, H. & Knoblich, G. Joint action: bodies and minds moving together. *Trends Cogn. Sci.* **10**, 70–6 (2006).
2. Schmidt, R. C., Fitzpatrick, P. A., Bienvenu, M. & Amazeen, P. G. A Comparison of Intra- and Interpersonal Interlimb Coordination: Coordination Breakdowns and Coupling Strength. *J. Exp. Psychol. Hum. Percept. Perform.* **24**, 884–900 (1998).
3. Konvalinka, I., Vuust, P., Roepstorff, A. & Frith, C. D. Follow you, follow me: Continuous mutual prediction and adaptation in joint tapping. *Q. J. Exp. Psychol.* **63**, 2220–2230 (2010).
4. Masumoto, J. & Inui, N. Two heads are better than one: both complementary and synchronous strategies facilitate joint action. *J. Neurophysiol.* **109**, 1307–1314 (2012).
5. Masumoto, J. & Inui, N. Motor control hierarchy in joint action that involves bimanual force production system controls force production and timing simultaneously at three levels of a motor control hierarchy in a joint action that involves bimanual force production: a top level. *J. Neurophysiol.* **113**, 3736–3743 (2015).
6. Mojtahedi, K., Fu, Q. & Santello, M. On the Role of Physical Interaction on Performance of Object Manipulation by Dyads. *Front. Hum. Neurosci.* **11**, 533 (2017).
7. Riley, M. A., Richardson, M. J., Shockley, K. & Ramenzoni, V. C. Interpersonal synergies. *Front. Psychol.* **2**, 38 (2011).
8. Ramenzoni, V. Effects of joint task performance on interpersonal postural coordination. (2008).
9. Reed, K. B. & Peshkin, M. A. Physical collaboration of human-human and human-robot teams. *IEEE Trans. Haptics* **1**, 108–120 (2008).
10. Carpenter, M. B. The Co-ordination and Regulation of Movements. *J. Neuropathol. Exp. Neurol.* **27**, 348 (1968).
11. Latash, M. L., Scholz, J. P. & Schönner, G. Toward a new theory of motor synergies. *Motor Control* **11**, 276–308 (2007).
12. Latash, M. L. The bliss (not the problem) of motor abundance (not redundancy). *Exp. Brain Res.* **217**, 1–5 (2012).
13. Bernshteĭn, N. A. *The co-ordination and regulation of movements.* (Pergamon Press, 1967).
14. Schmidt, R. C. & Turvey, M. T. Phase-entrainment dynamics of visually coupled rhythmic movements. *Biol. Cybern.* **70**, 369–76 (1994).
15. Schmidt, R., Carello, C., Experimental, M. T.-J. of & 1990, U. Phase transitions and critical fluctuations in the visual coordination of rhythmic movements between people. *psycnet.apa.org* (1990).
16. Newman-Norlund, R. D., Bosga, J., Meulenbroek, R. G. J. & Bekkering, H. Anatomical substrates of cooperative joint-action in a continuous motor task: Virtual lifting and balancing. *Neuroimage* **41**, 169–177 (2008).
17. Bosga, J. & Meulenbroek, R. G. J. Joint-Action Coordination of Redundant Force Contributions in a Virtual Lifting Task. *Motor Control* **11**, 235–258 (2007).
18. Ganesh, G. *et al.* Two is better than one: Physical interactions improve motor performance in humans. *Sci. Rep.* **4**, 3824 (2015).
19. Kelso, J. A., Southard, D. L. & Goodman, D. On the coordination of two-handed

- movements. *J. Exp. Psychol. Hum. Percept. Perform.* **5**, 229–38 (1979).
20. Schmidt, R. C., Richardson, M. J., Arsenault, C. & Galantucci, B. Visual Tracking and Entrainment to an Environmental Rhythm. *J. Exp. Psychol. Hum. Percept. Perform.* **33**, 860–870 (2007).
 21. Van der Wel, R. P. R. D., Knoblich, G. & Sebanz, N. Let the Force Be With Us: Dyads Exploit Haptic Coupling for Coordination. *J. Exp. Psychol. Hum. Percept. Perform.* **37**, 1420–1431 (2011).
 22. Keller, P. E. & Repp, B. H. Multilevel coordination stability: Integrated goal representations in simultaneous intra-personal and inter-agent coordination. *Acta Psychol. (Amst)*. **128**, 378–386 (2008).
 23. Gelfand, I. M. & Latash, M. L. On the problem of adequate language in motor control. *Motor Control* **2**, 306–13 (1998).
 24. Turvey, M. T. Coordination. *Am. Psychol.* **45**, 938–953 (1990).
 25. Koh, K. *et al.* The role of tactile sensation in online and offline hierarchical control of multi-finger force synergy. *Exp. Brain Res.* **233**, 2539–2548 (2015).
 26. Solnik, S., Qiao, M. & Latash, M. L. Effects of visual feedback and memory on unintentional drifts in performance during finger-pressing tasks. *Exp. Brain Res.* **235**, 1149–1162 (2017).
 27. Solnik, S., Reschechtko, S., Wu, Y.-H., Zatsiorsky, V. M. & Latash, M. L. Force-stabilizing synergies in motor tasks involving two actors. *Exp. Brain Res.* **233**, 2935–2949 (2015).
 28. Slifkin, A. B., Vaillancourt, D. E. & Newell, K. M. Intermittency in the Control of Continuous Force Production. *J. Neurophysiol.* **84**, 1708–1718 (2000).
 29. Sosnoff, J. J. & Newell, K. M. Intermittency of Visual Information and the Frequency of Rhythmical Force Production. *J. Mot. Behav.* **37**, 325–336 (2005).
 30. Hu, X. & Newell, K. M. Aging, visual information, and adaptation to task asymmetry in bimanual force coordination Downloaded from. *J Appl Phy-siol* **111**, 1671–1680 (2011).
 31. Scholz, J. P. & Schöner, G. The uncontrolled manifold concept: identifying control variables for a functional task. *Exp. Brain Res.* **126**, 289–306 (1999).
 32. Diederich, A. Intersensory Facilitation of Reaction Time: Evaluation of Counter and Diffusion Coactivation Models. *J. Math. Psychol.* **39**, 197–215 (1995).
 33. Bosga, J. & Meulenbroek, R. G. J. *Joint-Action Coordination of Redundant Force Contributions in a Virtual Lifting Task. Motor Control* **11**, (2007).
 34. Black, D. P., Riley, M. A. & McCord, C. K. Synergies in intra- and interpersonal interlimb rhythmic coordination. *Motor Control* **11**, 348–73 (2007).
 35. Reed, K. B. *et al.* Haptic cooperation between people, and between people and machines. in *IEEE International Conference on Intelligent Robots and Systems* 2109–2114 (IEEE, 2006). doi:10.1109/IROS.2006.282489
 36. Ganesh, G., Kawato, M., Burdet, E., Yoshioka, T. & Takagi, A. Physically interacting individuals estimate the partner’s goal to enhance their movements. *Nat. Hum. Behav.* (2017). doi:10.1038/s41562-017-0054
 37. Sallnäs, E.-L., Rasmus-Gröhn, K. & Sjöström, C. Supporting presence in collaborative environments by haptic force feedback. *ACM Trans. Comput. Interact.* **7**, 461–476 (2000).
 38. Gentry, S. Dancing cheek to cheek: Haptic communication between partner dancers and swing as a finite state machine. (2005).
 39. Latash, M. L., Scholz, J. P. & Schöner, G. Motor control strategies revealed in the

- structure of motor variability. *Exerc. Sport Sci. Rev.* **30**, 26–31 (2002).
40. Gorniak, S. L., Zatsiorsky, V. M. & Latash, M. L. Hierarchies of synergies: An example of two-hand, multi-finger tasks. *Exp. Brain Res.* **179**, 167–180 (2007).
 41. Gorniak, S. L., Zatsiorsky, V. M. & Latash, M. L. Emerging and disappearing synergies in a hierarchically controlled system. *Exp. Brain Res.* **183**, 259–270 (2007).
 42. Fine, J. M. & Amazeen, E. L. Interpersonal Fitts' law: when two perform as one. *Exp. Brain Res.* **211**, 459–469 (2011).
 43. Sawers, A. & Ting, L. H. Perspectives on human-human sensorimotor interactions for the design of rehabilitation robots. *J. Neuroeng. Rehabil.* **11**, 142 (2014).
 44. Takagi, A., Beckers, N. & Burdet, E. Motion plan changes predictably in dyadic reaching. *PLoS One* **11**, e0167314 (2016).
 45. Beckers, N., Keemink, A., van Asseldonk, E. & van der Kooij, H. Haptic human-human interaction through a compliant connection does not improve motor learning in a force field. in *Lecture Notes in Computer Science (including subseries Lecture Notes in Artificial Intelligence and Lecture Notes in Bioinformatics)* **10893 LNCS**, 333–344 (2018).
 46. Takagi, A., Usai, F., Ganesh, G., Sanguineti, V. & Burdet, E. Haptic communication between humans is tuned by the hard or soft mechanics of interaction. *PLoS Comput. Biol.* **14**, e1005971 (2018).
 47. Wahn, B., Karlinsky, A., Schmitz, L. & König, P. Let's Move It Together: A Review of Group Benefits in Joint Object Control. *Front. Psychol.* **9**, 918 (2018).
 48. Wahn, B., Kingstone, A. & König, P. Group benefits in joint perceptual tasks—a review. *Ann. N. Y. Acad. Sci.* **1426**, 166–178 (2018).
 49. Tatti, F. & Baud-Bovy, G. Force sharing and other collaborative strategies in a dyadic force perception task. *PLoS One* **13**, e0192754 (2018).
 50. Sylos-Labini, F., d'Avella, A., Lacquaniti, F. & Ivanenko, Y. Human-Human Interaction Forces and Interlimb Coordination During Side-by-Side Walking With Hand Contact. *Front. Physiol.* **9**, 179 (2018).
 51. Helbig, H. B. & Ernst, M. O. Optimal integration of shape information from vision and touch. *Exp. Brain Res.* **179**, 595–606 (2007).
 52. on Coordination of Two-Handed Movement.Pdf.
 53. Shim, J. K., Latash, M. L. & Zatsiorsky, V. M. Prehension synergies: trial-to-trial variability and hierarchical organization of stable performance. *Exp. Brain Res.* **152**, 173–184 (2003).
 54. Brown, C. Y. & Asada, H. H. Inter-finger coordination and postural synergies in robot hands via mechanical implementation of principal components analysis. *IEEE Int. Conf. Intell. Robot. Syst.* 2877–2882 (2007). doi:10.1109/IROS.2007.4399547
 55. Uno, Y., Kawato, M. & Suzuki, R. Formation and control of optimal trajectory in human multijoint arm movement. *Biol. Cybern.* **61**, 89–101 (1989).
 56. Todorov, E. & Jordan, M. I. Optimal feedback control as a theory of motor coordination. *Nat. Neurosci.* **5**, 1226–1235 (2002).
 57. Diedrichsen, J., Shadmehr, R. & Ivry, R. B. The coordination of movement: optimal feedback control and beyond. *Trends Cogn. Sci.* **14**, 31–39 (2010).
 58. Laczko, J., Jaric, S., Johansson, H. & Latash, M. L. Experimental Brain Research, Volume 143, Number 1 - SpringerLink. *Exp. Brain ...* (2002).
 59. Sallnäs, E.-L. & Zhai, S. Collaboration meets Fitts' law : Passing Virtual Objects with

- and without Haptic Force Feedback. *Interact* 97–104 (2003).
60. Basdogan, C., Ho, C.-H., Srinivasan, M. A. & Slater, M. An experimental study on the role of touch in shared virtual environments. *ACM Trans. Comput. Interact.* **7**, 443–460 (2000).
 61. Knoblich, G. & Jordan, J. S. Action Coordination in Groups and Individuals: Learning Anticipatory Control. *J. Exp. Psychol. Learn. Mem. Cogn.* **29**, 1006–1016 (2003).
 62. Reed, K. *et al.* *Haptically Linked Dyads Are Two Motor-Control Systems Better Than One?* (2006).
 63. Gentry, S., Feron, E. & Murray-Smith, R. Human-human haptic collaboration in cyclical Fitts' tasks. in *2005 IEEE/RSJ International Conference on Intelligent Robots and Systems, IROS* 710–715 (2005). doi:10.1109/IROS.2005.1545064
 64. Latash, M. L., Gorniak, S. & Zatsiorsky, V. M. Hierarchies of Synergies in Human Movements. *Kinesiology (Zagreb)*. **40**, 29–38 (2008).
 65. Shim, J. K., Latash, M. L. & Zatsiorsky, V. M. The human central nervous system needs time to organize task-specific covariation of finger forces. *Neurosci. Lett.* **353**, 72–4 (2003).
 66. Shim, J. K., Lay, B. S., Zatsiorsky, V. M. & Latash, M. L. Age-related changes in finger coordination in static prehension tasks. *J. Appl. Physiol.* **97**, 213–224 (2004).
 67. Karol, S. *et al.* Multi-finger pressing synergies change with the level of extra degrees of freedom. *Exp. Brain Res.* **208**, 359–367 (2011).
 68. Latash, M. L. *Synergy*. (Oxford University Press, 2008).
 69. Latash, M. L., Gorniak, S. & Zatsiorsky, V. M. Hierarchies of Synergies in Human Movements The Problem of Motor Redundancy The Principle of Abundance Synergy – an Operational Definition. (1998).
 70. Ranganathan, R. & Newell, K. M. Motor synergies: feedback and error compensation within and between trials. *Exp. Brain Res.* **186**, 561–570 (2008).
 71. Bizzi, E. & Cheung, V. C. K. The neural origin of muscle synergies. *Front. Comput. Neurosci.* **7**, 51 (2013).
 72. Jian, J. MODELING OF HUMAN MOTOR CONTROL AND ITS APPLICATION IN HUMAN INTERACTION Gra in partial fulfillment of the requireme. (2017).
 73. Mojtahedi, K. Assessing Performance, Role Sharing, and Control Mechanisms in Human-Human Physical Interaction for Object Manipulation Human-Human Physical Interaction View project. (2017). doi:10.13140/RG.2.2.18390.55366
 74. Latash, M. L., Scholz, J. P. & Schönér, G. Motor Control Strategies Revealed in the Structure of Motor... : Exercise and Sport Sciences Reviews. *Exerc. Sport Sci. Rev.* **30**, 26–31 (2002).
 75. Shapkova, E. Y., Shapkova, A. L., Goodman, S. R., Zatsiorsky, V. M. & Latash, M. L. Do synergies decrease force variability? A study of single-finger and multi-finger force production. *Exp. brain Res.* **188**, 411–25 (2008).
 76. Chatfield, C., Bendat, J. S. & Piersol, A. G. Random Data: Analysis and Measurement Procedures. *J. R. Stat. Soc. Ser. A* **150**, 167 (2006).
 77. Franklin, D. W. & Wolpert, D. M. Computational mechanisms of sensorimotor control. *Neuron* **72**, 425–442 (2011).
 78. Ernst, M. O. & Banks, M. S. Integrate Visual and Haptic_2002.Pdf. **415**, 429–433 (2002).
 79. Deneve, S. & Pouget, A. Bayesian multisensory integration and cross-modal spatial links. *J. Physiol.* **98**, 249–258 (2004).

80. Rowland, B. A. & Stein, B. E. Multisensory integration produces an initial response enhancement. *Front. Integr. Neurosci.* **1**, 4 (2007).
81. Byadarhaly, K. V., Perdoor, M. C. & Minai, A. A. A modular neural model of motor synergies. *Neural Networks* **32**, 96–108 (2012).
82. Goodman, S. R. & Latash, M. L. Feed-forward control of a redundant motor system. *Biol. Cybern.* **95**, 271–280 (2006).
83. Crevecoeur, F., Giard, T., Thonnard, J.-L. & Lefèvre, P. Adaptive control of grip force to compensate for static and dynamic torques during object manipulation. *J. Neurophysiol.* **106**, 2973–2981 (2011).
84. Zatsiorsky, V. M., Li, Z. M. & Latash, M. L. Coordinated force production in multi-finger tasks: Finger interaction and neural network modeling. *Biol. Cybern.* **79**, 139–150 (1998).
85. Shim, J. K. *et al.* Tactile feedback plays a critical role in maximum finger force production. *J. Biomech.* **45**, 415–420 (2012).
86. Latash, M. L., Shim, J. K., Smilga, A. V. & Zatsiorsky, V. M. A central back-coupling hypothesis on the organization of motor synergies: a physical metaphor and a neural model. *Biol. Cybern.* **92**, 186–191 (2005).
87. Li, Z. M., Zatsiorsky, V. M., Latash, M. L. & Bose, N. K. Anatomically and experimentally based neural networks modeling force coordination in static multi-finger tasks. *Neurocomputing* **47**, 259–275 (2002).
88. Rack, P. Control of Human Voluntary Movement. *J. Neurol. Neurosurg. Psychiatry* **50**, 1090–1091 (2008).
89. Hajian, A. Z. & Howe, R. D. Identification of the Mechanical Impedance at the Human Finger Tip. *J. Biomech. Eng.* **119**, 109 (1997).
90. Paillard, J. Fast and slow feedback loops for the visual correction of spatial errors in a pointing task: a reappraisal. *Can. J. Physiol. Pharmacol.* **74**, 401–17 (1996).
91. Ward, L. M. *Dynamical Cognitive Science.* (2002).
92. Greenwood, P. E., Ward, L. M., Russell, D. F., Neiman, A. & Moss, F. Stochastic Resonance Enhances the Electrosensory Information Available to Paddlefish for Prey Capture. *Phys. Rev. Lett.* **84**, 4773–4776 (2000).
93. Colley, I. D. & Dean, R. T. Origins of 1/f noise in human music performance from short-range autocorrelations related to rhythmic structures. *PLoS One* **14**, e0216088 (2019).
94. Jiang, W., Jiang, H. & Stein, B. E. Two Corticotectal Areas Facilitate Multisensory Orientation Behavior. *J. Cogn. Neurosci.* **14**, 1240–1255 (2002).
95. Rowland, B. A. Multisensory integration produces an initial response enhancement. *Front. Integr. Neurosci.* **1**, (2008).
96. Soderstrom, T. & Stoica, P. System identification. *Prencite Hall Intemational* (1997).
97. Goldberg, L. R. The Development of Markers for the Big-Five Factor Structure. *Psychol. Assess.* **4**, 26–42 (1992).